Master's thesis

NTNU
Norwegian University of Science and Technology
Faculty of Natural Sciences
Department of Materials Science and Engineering

Vegard Aulie

Dispersion and dissolution of alumina in cryolite melts

Impact of sulfur and carbon on dissolution behavior in see through cell

Master's thesis in Chemical Engineering and Biotechnology
Supervisor: Kristian Etienne Einarsrud
Co-supervisor: Espen Sandnes
July 2021

NTNU
Kunnskap for en bedre verden

Vegard Aulie

Dispersion and dissolution of alumina in cryolite melts

Impact of sulfur and carbon on dissolution behavior in see through cell

Master's thesis in Chemical Engineering and Biotechnology
Supervisor: Kristian Etienne Einarsrud
Co-supervisor: Espen Sandnes
July 2021

Norwegian University of Science and Technology
Faculty of Natural Sciences
Department of Materials Science and Engineering

NTNU
Norwegian University of
Science and Technology

Acknowledgment

First, I wany to thank Professor Kristian Etienne Einarsrud and Associate Professor Espen Sandnes for facilitating this Master's project so I could work from home and travel to Trondheim for the laboratory work, and for always seeing solutions where I could only see problems.

I would like to thank everyone who has helped me with experiments, PhD candidate Luis Bracamonte, PhD candidate Nikolina Stanic, PhD candidate Omar Awayssa and PhD candidate Erik Aas Koren. Thank you to PhD candidate Sindre Engzelius Gylver for helping me with the image processing.

I also want to acknowledge Alcoa Mosjøen for the opportunity to work at their plant and conducting experiments there the summer of 2019.

This project is partly funded by the SFI Metal Production, (Centre for Research-based Innovation, 237738). I gratefully acknowledge the financial support from the Research Council of Norway and the partners of the SFI Metal Production. I am also grateful to Alcoa, Hydro and Sintef for providing me with necessary materials for my project.

Finally thank you to my family and friends for keeping my spirits up throughout the semester. Special thanks to my parents for motivating me and to Christoffer for helpful feedback.

Abstract

Aluminium is produced industrially using the Hall-Herôult method. This method produces liquid aluminium from aluminium oxide (called alumina) and carbon in a molten cryolite bath. This process requires high temperature and has a high energy demand. When 'cold' alumina is added to the molten cryolite, which typically has a temperature of 960°C, it doesn't immediately dissolve but instead form an agglomeration on the surface of the cryolite, a process called raft formation. Improving the feeding process is necessary to increase production in aluminium smelters. The influence of sulfur and carbon on aluminium production are well discussed topics, but their quantitative influence on raft formation and dissolution has not been investigated.

Three different melt experiments in a see through cell was performed on an industrial bath with excess lithium fluoride to investigate possible influence from sulfur and carbon on alumina dissolution. A set of normal experiments was done to establish a standard dissolution time for comparison. Experiments with sodium sulfate mixed in alumina were done to examine influence of sulfur. Experiments with carbon mixed into the bath was done to examine influence of carbon.

In addition a method for automatic processing of videos taken from the experiments was attempted. ImageJ was utilized as the processing program, and a working method was found which used the treshold function to distinguish raft and cryolite. Due to problems with lighting conditions it was hard to extract quantitative data based on the automatic processing alone, and visual observations had to be used to find dissolution times. The automatic prosessing method should be investigated further. Based on the semi-qualitative results found in this project, sulfur was found to make the dissolution process faster while carbon made the dissolution process go slower. Further investigation on carbon as a dissolution factor could improve operations.

Sammendrag

Aluminium blir produsert industrielt ved hjelp av Hall-Herôult metoden. Denne metoden produserer flytende aluminium fra aluminiumoksid (kalt alumina) og karbon i ett bad med flytende kryolitt. Denne prosessen krever høy temperatur og har ett høyt energikrav. Når kald alumina blir tilsatt flytende kryolitt, som typisk har en temperatur på 960° C, vil den ikke oppløses umiddelbart men heller danne en agglomerasjon på overflaten av kryolitten, en prosess som kalles flåtedannelse. Å forbedre tilsettelsesprosessen er nødvendig for å øke produksjonen i aluminiumsmelteverk. Påvirkningen av svovel og karbon på aluminiumsproduksjonen er vel diskuterte emner, men deres kvantitative påvirkning på flåtedannelse og oppløsning har ikke blitt utforsket.

Tre forskjellige smelteeksperimenter i en gjennomsiktig celle ble gjennomført i ett industribad med ekstra litiumfluorid for å undersøke mulig påvirkning fra svovel og karbon på aluminaoppløsning. Ett sett med vanlige eksperimenter ble gjennomført for å danne en standard oppløsningstid for sammenligning. Eksperimenter med natriumsulfat blandet med alumina ble gjort for å undersøke svovels innflytelse. Eksperimenter med karbon blandet inn i indudstribad ble gjort for å undersøke påvirkningen til karbon.

En metode for automatisk prosessering av videoene fra eksperimentene ble laget. ImageJ ble brukt som prosesseringsprogram, og en fungerende metode ble funnet ved bruk av en 'terskel' funksjon for å skille flåte og kryolitt. På grunn av problemer med lysforholdene var det vanskelig å hente ut kvantitative data basert på den automatiske prosesseringen alene, så visuelle observasjoner ble tatt i bruk for å bestemme oppløsningstider. Den automatiske prosesseringsmetoden burde utforskes videre. Basert på semi-kvalitative resultater funnet i dette prosjektet vil svovel føre til en raskere oppløsningsprosess, mens karbon fører til en tregere oppløsningsprosess. Videre analyse på karbon som en oppløsningsfaktor kan hjelpe med å forbedre aluminiumsproduksjon.

Contents

Acknowledgment i

Abstract ii

Sammendrag iii

List of Figures vi

List of Tables viii

1 Background and Introduction 1
- 1.1 The Hall-Hêroult process . . . 1
- 1.2 Alumina Dissolution . . . 2
- 1.3 Objectives and scope of work . . . 3

2 Litterature review 4
- 2.1 Sulphur . . . 4
- 2.2 Carbon . . . 7
- 2.3 Review of experiments with see through oven . . . 12

3 Experimental 22
- 3.1 Setup . . . 22
- 3.2 Cryolite mixture . . . 24
- 3.3 Materials . . . 24
- 3.4 Initial Experiments . . . 25
- 3.5 Experiments conducted . . . 25
  - 3.5.1 Establishing a standard . . . 25
  - 3.5.2 Sulfur . . . 25
  - 3.5.3 Carbon . . . 26
  - 3.5.4 Table of the experiments conducted . . . 26
- 3.6 Image processing . . . 26
- 3.7 Dissolution times . . . 28

4 Results 29
- 4.1 Initial experiments . . . 29
  - 4.1.1 Dissolution of Primary Alumina . . . 29
  - 4.1.2 Dissolution of Secondary Alumina . . . 30
- 4.2 Establishing a standard . . . 33
- 4.3 Sulfur . . . 38
- 4.4 Carbon . . . 47

4.5 Dissolution times 54

5 Discussion **56**
5.1 Experimental setup 56
5.2 Image processing 56
5.3 Initial experiments 57
5.4 Establishing a standard 57
5.5 Sulfur 57
5.6 Carbon 58
5.7 Uncertainties 58

6 Conclusion and Further work **60**

7 References **61**

List of Figures

1.1 Sketch of cell . . . 2
2.1 Dissolution curves for alumina . . . 4
2.2 Setup by Meirbekova . . . 6
2.3 Graph from Meirbekova . . . 6
2.4 Setup by Meirbekova . . . 7
2.5 Table by Meirbekova . . . 7
2.6 Carbon dust formation . . . 8
2.7 Dissolution experiment on industrial cell with carbon dust . . . 9
2.8 Dissolution experiment on industrial cell . . . 10
2.9 Size distribution of carbon dust particles . . . 11
2.10 Setup used by Bugnion . . . 11
2.11 Carbon dust levels . . . 12
2.12 Setup used by Haupin . . . 13
2.13 Setup used by Yang . . . 14
2.14 Primary alumina dissolution by Yang . . . 15
2.15 Secondary alumina dissolution by Yang . . . 16
2.16 Setup used by Gao . . . 17
2.17 Dissolution experiments by Gao . . . 18
2.18 Picture of destroyed crucible . . . 19
2.19 Dissolution experiment done in Project work . . . 20
2.20 Setup used by Bracamonte . . . 21
3.1 Picture of the furnace used in the experiments. . . . 22
3.2 Crucible in oven . . . 23
3.3 Example of cropping . . . 27
3.4 Example of treshold . . . 28
4.1 Primary alumina dissolution experiment 02.06.2020 . . . 29
4.2 Secondary alumina dissolution experiment 12.05.2020 . . . 30
4.3 Secondary alumina dissolution experiment 02.06.2020 . . . 31
4.4 Standard dissolution experiment at 14.04.2021 . . . 33
4.5 Treshold from standard dissolution experiment at 14.04.2021 . . . 34
4.6 Graph14.04 . . . 35
4.7 Standard dissolution experiment at 16.04.2021 . . . 36
4.8 Treshold from standard dissolution experiment at 16.04.2021 . . . 37
4.9 Graph16.04 . . . 38
4.10 Sulfur dissolution experiment at 22.04.2021 . . . 39
4.11 Treshold from sulfur dissolution experiment at 22.04.2021 . . . 40
4.12 Graph22.04 . . . 41
4.13 Sulfur 2nd dissolution experiment at 03.06.2021 . . . 42
4.14 Treshold from 2nd sulfur dissolution experiment at 03.06.2021 . . . 43

4.15 Graph03.06-2 44
4.16 Sulfur 4th dissolution experiment at 03.06.2021 45
4.17 Treshold from 4th sulfur dissolution experiment at 03.06.2021 . . . 46
4.18 Graph03.06-4 47
4.19 Picture of crucible 26.05 48
4.20 Carbon dissolution experiment at 28.05.2021 49
4.21 Treshold from carbon dissolution experiment at 28.05.2021 50
4.22 Graph28.05 51
4.23 Carbon dissolution experiment at 01.06.2021 52
4.24 Treshold from carbon dissolution experiment at 01.06.2021 53
4.25 Graph01.06 54

List of Tables

3.1 Physical data for the main alumina used in this work given by the producer 25
3.2 Table presenting all the melt experiments done during the Master's project. 26
4.1 Dissolution times for standard experiments 54
4.2 Dissolution times for sulfur experiments 55
4.3 Dissolution times for carbon experiments 55

1 Background and Introduction

1.1 The Hall-Hêroult process

Aluminium is produced industrially using the Hall-Heroult method, which was discovered and patented by Charles Hall from USA and Paul Héroult from France independently of each other in 1886 [1]. Today it is the only method which is used to produce aluminium commercially[2]. Alumina (Al_2O_3) is dissolved in a bath mostly containing molten cryolite (Na_3AlF_6), and through an electrolytic reduction liquid aluminium is produced. The overall chemical reaction for the Hall-Héroult method is given as:

$$Al_2O_3(\text{diss}) + \frac{3}{2}C(\text{s}) \longrightarrow 2\,Al(\text{l}) + \frac{3}{2}CO_2(\text{g}), \tag{1.1}$$

where diss stands for dissolved, s stands for solid state, l stands for liquid state and g stands for gaseous state. At the cathode, $Al_3{}^+$ ions are reduced:

$$Al_3{}^+ + 3\,e^- \longrightarrow Al(\text{l}) \tag{1.2}$$

Liquid aluminium has a higher density than cryolite, and will thus form a liquid layer at the bottom of the cell. The anodes are made of carbon, and they are continually consumed during the process as they react with oxygen:

$$C(\text{s}) + 2\,O_2{}^- \longrightarrow CO_2(\text{g}) \tag{1.3}$$

In addition to being the raw material in the aluminium production, alumina serves several purposes [1]. Alumina is also a large part of the crust formed above the cryolite surface, which consists of frozen bath in addition to alumina. The crust acts as insulation for the molten bath. Additionally alumina is used as a filter for dangerous gases, such as HF, C_2F_4 and C_2F_6, which are produced from unwanted side reactions. This process is called dry scrubbing. Alumina that hasn't been dry scrubbed is called primary alumina, while after dry scrubbing its called secondary alumina. By feeding secondary alumina to the cell a lot of the fluorides are reintroduced to the cell.

Alumina is introduced to the cell using point feeders. These feeders consist of a crust breaker, which is used to create holes in the crust, and alumina is then fed from a chamber above the cell. 0.5-2 kg of alumina is added to the cell at each point feeder at intervals between 1-3 minutes. A sketch of a cell is provided in Figure 1.1. In addition to cryolite the bath of the cell also consists of several additives which influences cell operation. Melts often contain 4-6 mass% calcium fluoride, CaF_2,

6-13 mass% excess aluminium fluoride (AlF_3 and 2-4 mass%alumina [1]. Fluorides like LiF or MgF_2 could also be added. Further description of the solubility of alumina and it's reaction with cryolite and additives is given by Skybakmoen et al. [3].

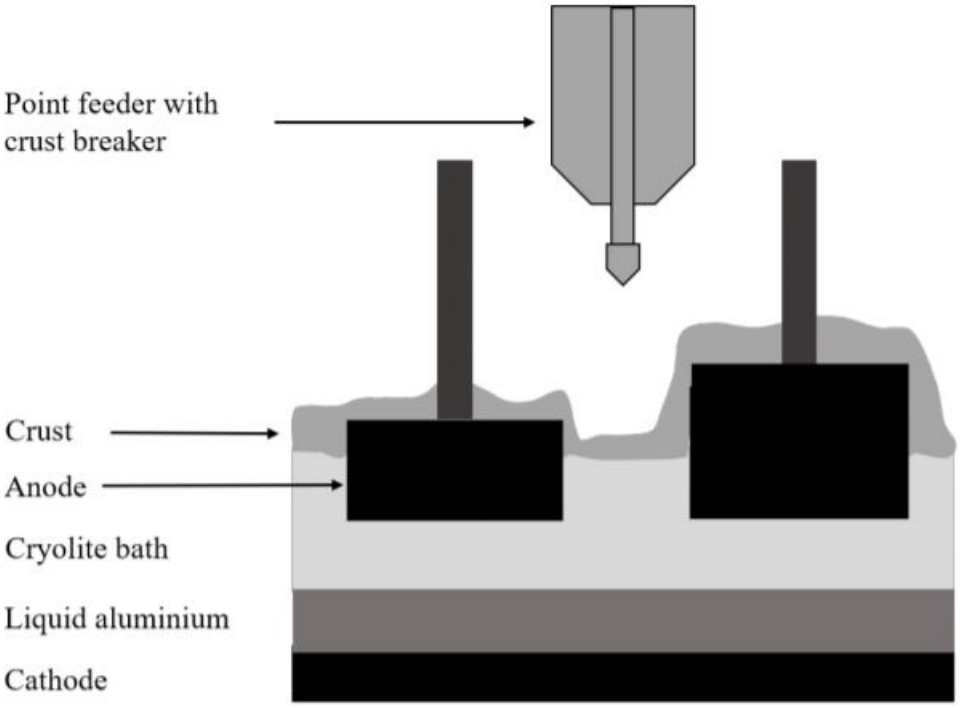

Figure 1.1: Sketch of a cell with prebaked anodes and point feeder taken from Åste Follo [4]

1.2 Alumina Dissolution

When alumina is fed to the cell everything doesn't immediately dissolve, but instead form rafts on the surface of the cryolite. This is because some bath freezes around the alumina powder when the cold alumina hits the warm bath with a temperature close to the liquidus. The rafts then proceed to float on the surface until they either heat up enough for the frozen bath to melt, a heat transfer controlled process which is followed by dissolution of the alumina powder, or the rafts could get completely covered by frozen bath and proceed to sink, where the raft will either dissolve in the cryolite bath or sink to the bottom of the cell and form a sludge layer under the liquid aluminium [2].

The concentration of alumina in the cell is an important factor for the aluminium production, both too high and low concentration is unfavorable for the output. A alumina concentration that is too high gives over-saturation in the molten bath, causing alumina to not dissolve in the bath. Too low concentration can lead to anode effects, where the cell does not get alumina to do the electrolysis and instead produce dangerous greenhouse gases by splitting cryolite. Keeping the alumina concentration between 2-4 % is typically the best for the cell [1].

1.3 Objectives and scope of work

To increase the production in aluminium smelters, aluminium cells are being operated at higher current, some as high as 600 kA. This results in increased cell sizes with more anodes, while the bath volume per anode doesn't increase. This results in lower interpolar distance and higher demands for dissolution and transport of alumina to the anodes. Better understanding of the mechanisms for alumina dispersion and dissolution are thus crucial for further progress in the aluminium industry.

One aim of this project is to establish a way to do repeatable experiments in the see-through cell by controlling the composition of the cryolite. Establishing a standard for these experiments is needed to investigate other factors that could be influencing alumina dissolution by making it possible to compare experiments where one factor is varied while other determined factors are unchanged.

Another aim of this project is to establish a method for automatic processing of videos taken from see through cell experiments. ImageJ will be utilized as the program for the video processing. The influence of sulfur in alumina and carbon in the cryolite on the dissolution times for alumina will be examined with this method in addition to the standard experiments.

To examine some factors to investigate a literature review on see through cell experiments was carried out. Some background theory was also gathered on the possible influence of sulfur and carbon on alumina dissolution.

2 Litterature review

Lavoie et al. [2] published a review of the feeding and dissolution factors of alumina in 2016 where they presented different factors and in what way they influence cell operations. Based on melt experiment done by Jain et. al [5], Lavoie could present their 4-step process of alumina dissolution for a poorly dispersed and dissolved alumina as shown in figure 2.1 [2].

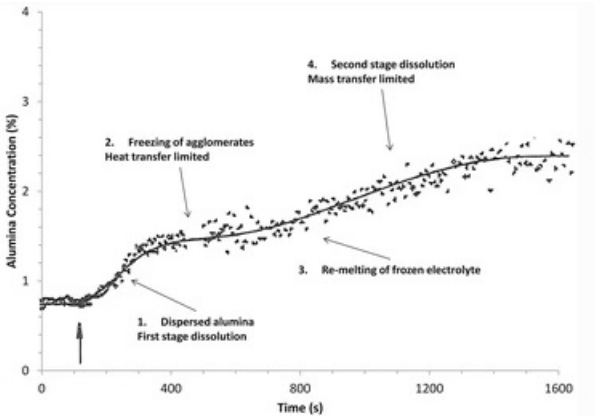

Figure 2.1: Dissolution curve for poorly dispersed and dissolved alumina in a cryolite melt based on melt experiment conducted by Jain et al.[5]. The arrows shows the 4 different steps in the dissolution process. Figure taken from Lavoie et al. [2].

2.1 Sulphur

Sulfur is the biggest impurity in the Hall-Heroult process, mainly entering through the cryolite mixture and anode [1]. The introduced sufhur will then exit the cell through the gas and get reintroduced by secondary alumina due to the dry-scrubbing system. The influence of anodes with a high content of sulfur has been investigated by Pietrzyk et al. [6] in a laboratory, and the results was indicating that current efficiency fell with increasing amount of sulfur content in the anode.

Fellner et al [7] examined the adsorption of SO_2 on alumina used in the aluminium industry in the temperature range of 15-120 °C. At low temperatures (less than 40 °C) SO_2 would bound reversibly to alumina, meaning it would desorb easily if heated. Meanwhile at temperatures above 80 °C, the temperature at which the dry scrubbing process is happening, the SO_2 would not desorb even at 250 °C. Lamb [8] also examined SO_2 adsorption in the dry scrubbing process, and found

that the adsorption of SO_2 drastically fell when HF was introduced in the same system. His tests on both laboratory scale and at aluminium plants showed that fluoride could displace adsorbed sulfur.

Hajasova [9] investigated the behavior of sulfur species in different baths based on chlorides and fluorides by using cyclic voltammetry, chronoamperometry and square wave voltammetry. Sodium sulfate was studied in a cryolite based electrolyte saturated with alumina. Sulfur was found to reach very low oxidation states in baths containing high amounts of AlF_3.

For the sulfur experiments planned in this project, sodium sulfate was chosen as the sulfur source. Sodium is present in the melt and sulfate is common in secondary alumina as described by Fellner et. al [7]. When introduced to cryolite , sodium sulfate will react with available carbon or aluminium as described by the equations in the appendix or decompose. The reactions are described by [10] and [11], and are written in the Appendix. These reactions are backed up by investigations on sulfur species in solidified cryolite melts by Ambrova et. al [12] and investigations on sulfur species in the anode gas by Oedegard et al. [13], which investigated what sulfur species that could be found in the cryolite melt and in the anode gas respectively.

Most the reactions described in [11] and [10] requires either carbon or aluminium to be available in the melt. But one reaction described has Na_2SO_4 reaction with cryolite as shown in equation 2.1.

$$3\,Na_2SO_4 + 2\,Na_3AlF_6 \longrightarrow 4\,Al_2(SO_4)_3 + 12\,NaF \tag{2.1}$$

The product created from this reaciton, $Al_2(SO_4)_3$, is described by Souza et al. [14] in their article about thermal decomposition of potassium alum ($KAl(SO_4)_2$. where$Al_2(SO_4)_3$ is an intermediate product that will end up as Al_2O_3 after decomposing. This indicates that SO_2 could be a by-product that escapes as gas.

Meirbekova et al. [15] investigated the effect of sulfur on the current efficiency in a laboratory cell as shown in figure 2.2. The experiment was done by continually adding sodium sulfate to the cryolite in an attempt to maintain a constant sulfur concentration at 1000 mg/kg (ppm). Alumina was added separately from the sulfate and the current efficiency for the experiment could be calculated based on how much aluminium that were produced. Their results are shown in figure 2.3, and it was found that the current efficiency was reduced by 1.1 percent per 100 mg/kg increase in sulfur concentration.

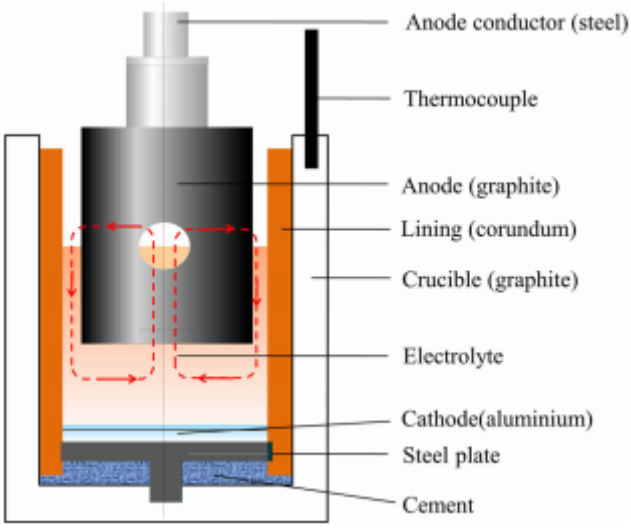

Figure 2.2: Schematic of the laboratory cell used by Meirbekova et al. [15].

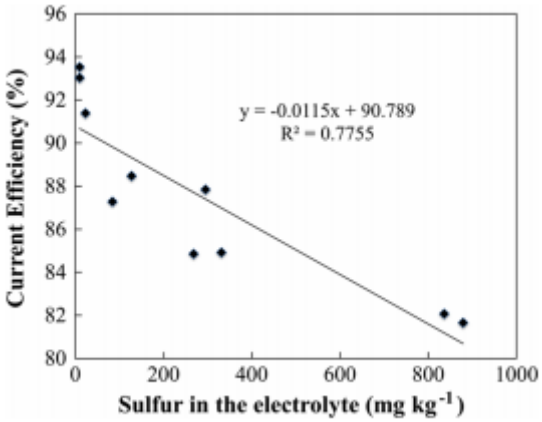

Figure 2.3: Graph from Meirbekova et al. [15] showing current efficiency as a function of the mean sulfur concentration in their cell at 0.8 A/cm^2

Meirbekova et al. [16] investigated the behavior of sulfur compounds in a cryolite-alumina melt. 600-800 ppm of sodium sulfate was in the bath at the start of each experiment. The amount of sulfur in the bath was measured with Inductive Coupled Plasma - Mass Spectrometry. Figure 2.4 shows the setup for the experiments,

and the results are presented in figure 2.5. The presence of carbon, alumina and electrolysis greatly decreased the half-life of sodium sulfate in the melt.

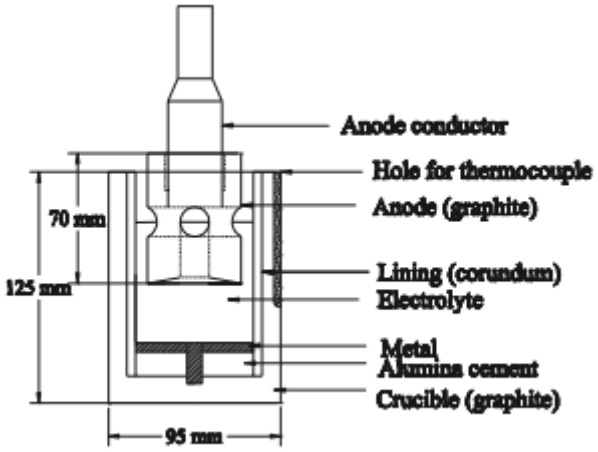

Figure 2.4: Schematic of the laboratory cell used by Meirbekova et al. [16]

Table II. Half-life of sodium sulfate at different conditions.

Carbon	Aluminium	Electrolysis	$T_{1/2}$ (min)
-	-	-	231
+	-	-	116
+	+	-	24
+	+	+	6.9

Figure 2.5: Table of half life of sodium sulfate from Meirbekova et al. [16]

It is obvious that sulfur has an impact on aluminium electrolysis, but it's influence the dissolution process of alumina has not been investigated. Given that full removal of sulfur is highly unlikely if not impossible, the direct influence of sulfur on alumina dissolution should be tested.

2.2 Carbon

Carbon dusting is a phenomenon that regularly occurs in the aluminium electrolysis process. Pietrzyk et al. [17] wrote a report on behalf of Hydro Aluminium discussing the effect of carbon dust in electrolyte. Figure 2.6 shows how carbon dust is formed at the anode-electrolyte interface. Carbon dust can be divided

into two groups: carbon dust dispersed throughout the electrolyte as tiny carbon particles and larger carbon particles floating on top of the electrolyte.

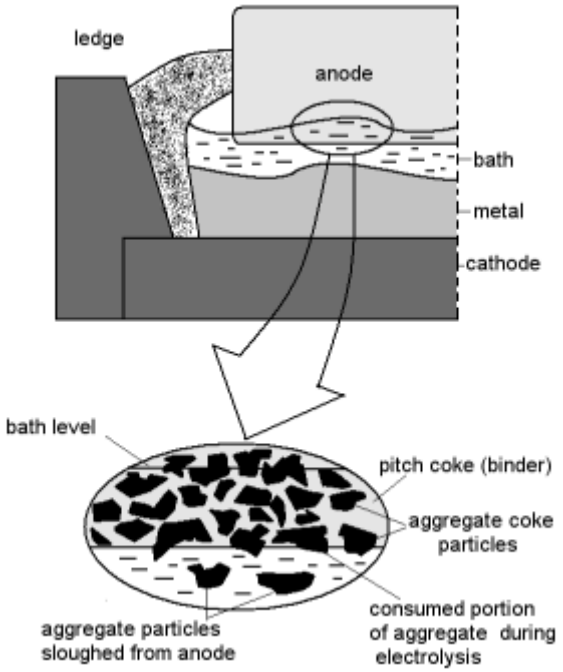

Figure 2.6: Figure showing formation of carbon dust at the anode in aluminium electrolysis from [17]

Carbon dust in industrial cells was experienced by both Follo [4] and Aulie [18] in their dissolution experiments performed at Alcoa Mosjøen in 2018 and 2019 respectively. As can be seen from figures 2.7 and 2.8 carbon dust was a big factor negatively impacting the alumina dissolution.

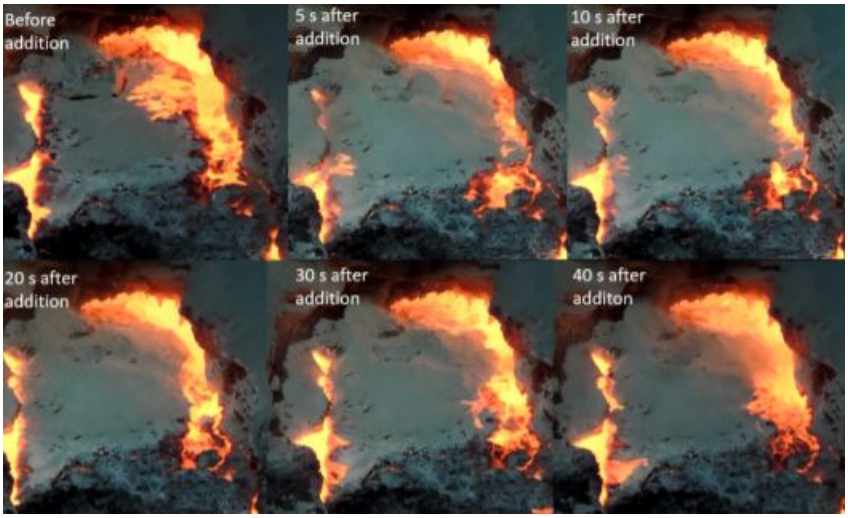

Figure 2.7: Figure showing a dissolution experiment done in an industrial cell with a lot of carbon dust at Alcoa Mosjøen. Experiment done by Åste Follo.

Figure 2.8: Figure showing a dissolution experiment done in an industrial cell at Alcoa Mosjøen. Experiment done by Vegard Aulie

Fossnæs et al. [19] investigated the size distribution of carbon particles and amount of carbon by gathering bath samples from the entire bath depth of ovens at Hydro Årdal. The samples were examined with a microscopic gravimetric oxidation analysis. Figure 2.9 shows the size distribution of dispersed carbon particles gathered from one of the ovens in the study.

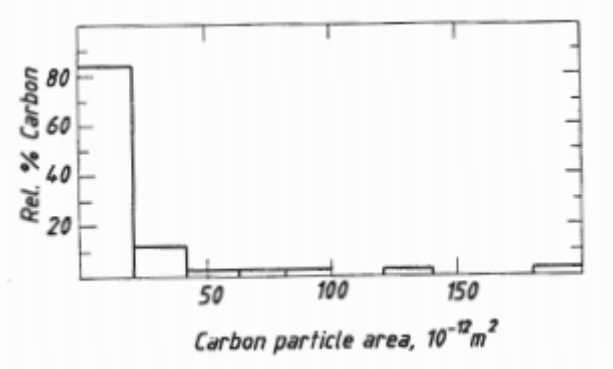

Figure 2.9: Figure showing the size distribution of carbon dust particles in a oven from [19]

Bugnion et al. [20] investigated the effect of carbon dust on the electrical resistivity of a cryolite bath by running experiments on a tube-type cell as shown in figure 2.10. A given wt % of carbon was given to each bath tested. They found that the bath resistivity increased 70 % when measured in a bath with 1.01 % carbon compared with one with 0.06 % carbon. An increase from 0.06 % carbon to 0.16% resulted in a 13% increase in resistivity.

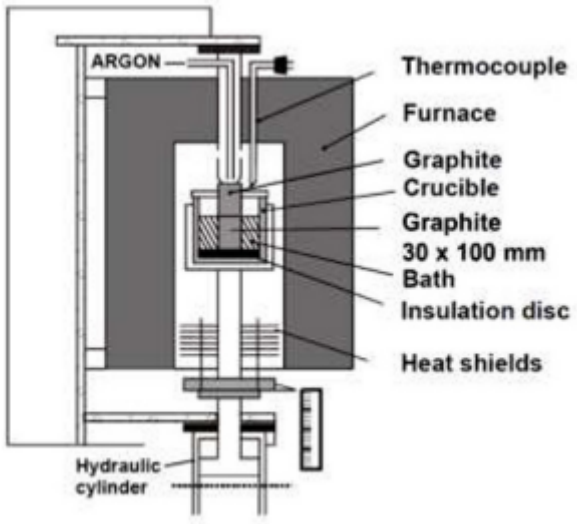

Figure 2.10: Schematic of the laboratory cell used by Bugnion et al. [20]

Dechent et al. [21] investigated the effect of carbon dust on anode changes in

industrial cells in the TRIMET Hamburg Smelter. Their hypothesis was that certain parameters, such as carbon dust level of the cell, would impact the spike formation on the anodes after they are changed. A spike is a deformation or protrusion on the anode, which in turn negatively impacts anode performance. Dechent could not find any correlation between carbon dust level in the tap hole or anode with spike formation. Figure 2.11

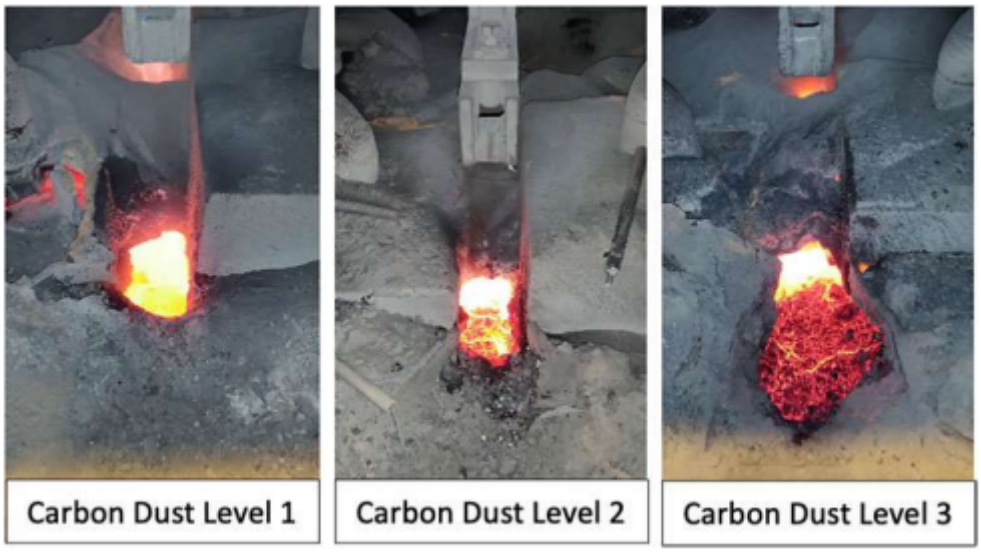

Figure 2.11: Figure showing carbon dust levels in the tap hole from [21]. Level 1 shows a tap hole with no carbon dust, level 2 shows a low amount of carbon dust while level 3 shows a high amount.

A lot of factors indicate that carbon dust has a negative impact on the alumina dissolution. However there has not been conducted experiments resulting in quantitative data on alumina dissolution compared to level of carbon dust in a cell as far as the author knows. This is a topic that should be examined further due to how common carbon dust is in industrial cells.

2.3 Review of experiments with see through oven

Observational experiments on alumina dissolution in industrial cells and laboratory cells are easy to do but does not give all the necessary information about the dissolution procedure. As the alumina disappears from the cryolite surface it's difficult to tell if everything dissolved or if whole rafts of alumina sank without dissolving. To further understand the mechanisms of alumina dissolution knowledge

of what happens beneath the cryolite surface is important, and this can be acquired by utilizing a see-through cell. This section will review some observational experiments done on alumina dissolution by use of see-through cells.

Haupin et al. [22] performed experiments in a see-through cell in 1974, the first known use of a transparent cell to examine molten salt electrolysis, to examine the circulation of electrolyte, formation of gas bubbles and metal mist at different stages of electrolysis. They used the external heating furnace shown in Figure 2.12 and a cell which included a cathode and an anode made of graphite.

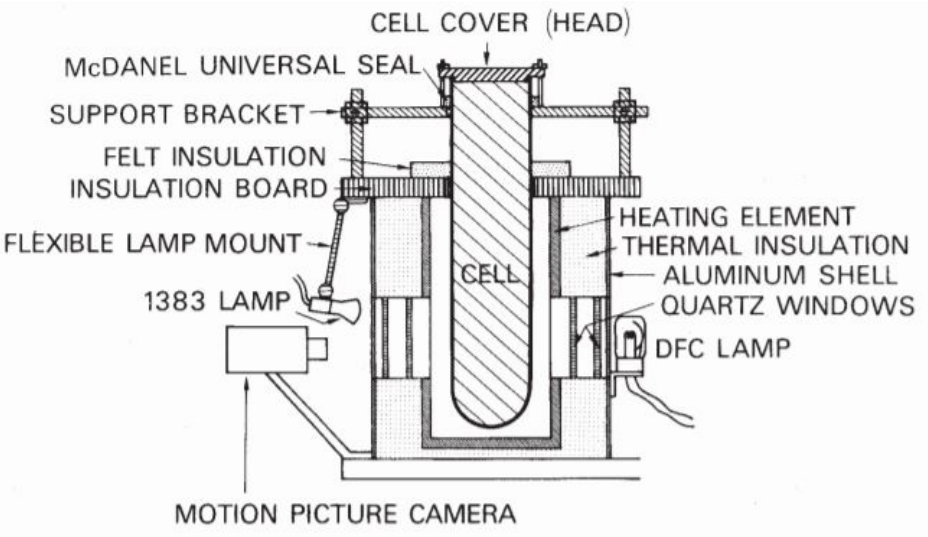

Figure 2.12: Figure of the setup used by Haupin et al.[22]

Yang et al. [23] used a see through cell with a high-purity quartz (SiO_2) crucible as shown in Figure 2.13 to observe the dissolution of alumina in a cryolite melt.

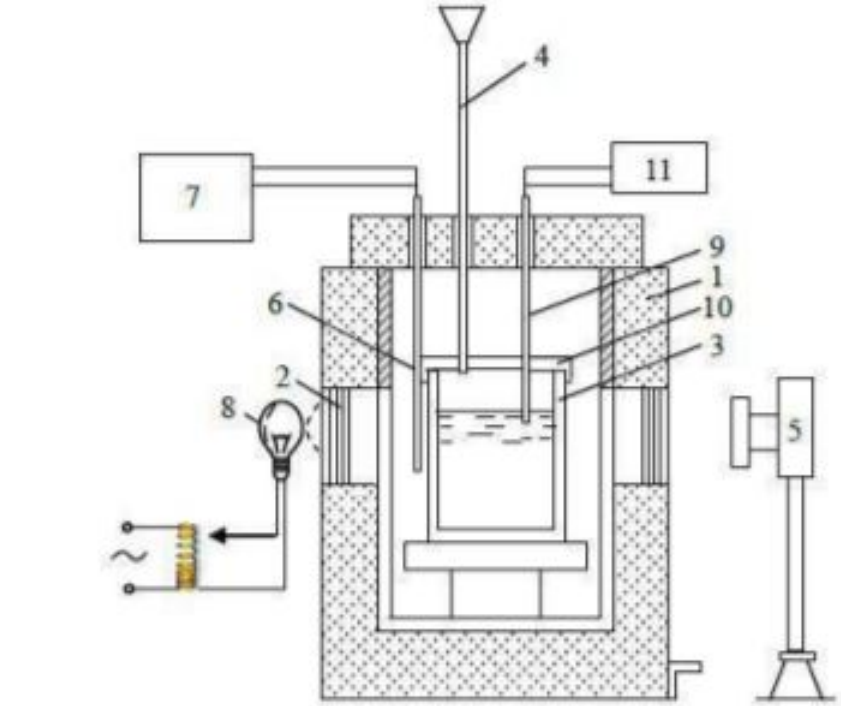

Figure 2.13: Figure of the setup used by Yang et al.[23]

The crucible contained 200 grams of cryolite at a liquidus temperature of 951°C with 4°C superheat. 2 grams of alumina was added to the cryolite for every experimental run. Figures 2.14 and 2.15 shows pictures of the dissolution of primary and secondary alumina respectively from [23]. For secondary alumina the crucible was clear 175 seconds after the alumina hit the cryolite surface, whilst for primary alumina the crucible was clear after 480 seconds. A crust is formed at the surface of the cryolite for both primary and secondary alumina. However, while the crust of secondary alumina dissolves at the surface, the crust of primary alumina doesn't completely dissolve but rather sinks to the bottom as can be seen in Figure 2.14.

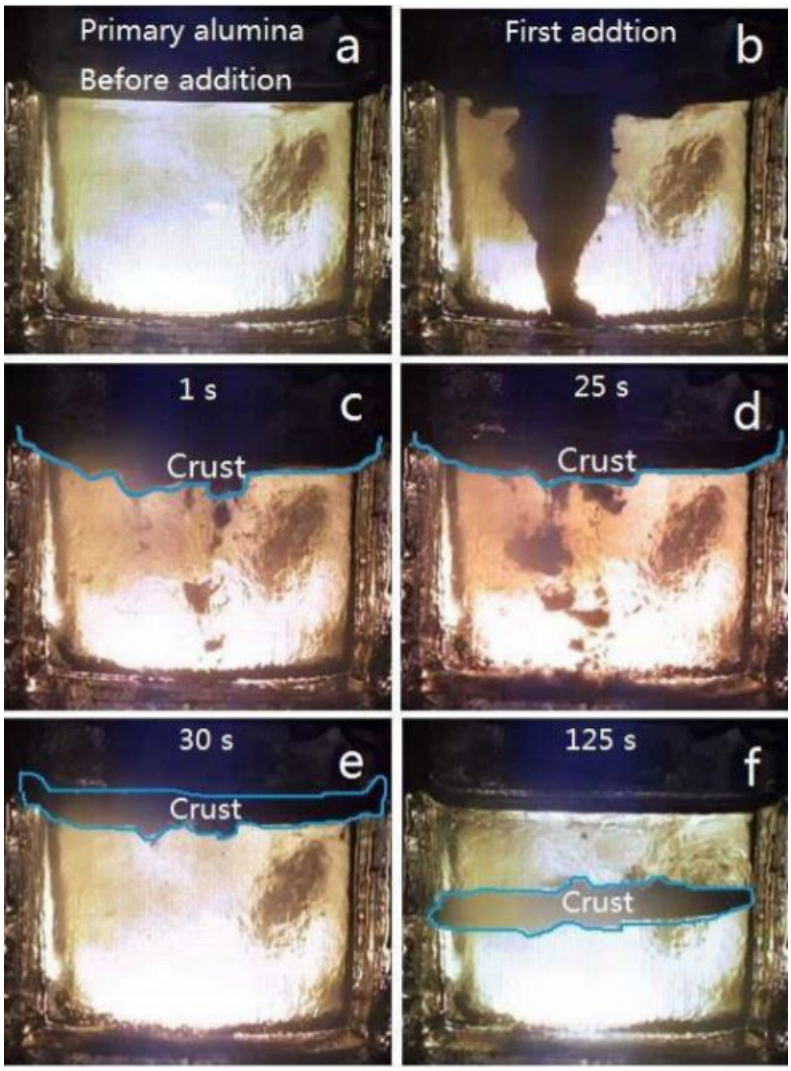

Figure 2.14: Dissolution of 2 grams of primary alumina in cryolite, taken from [23]

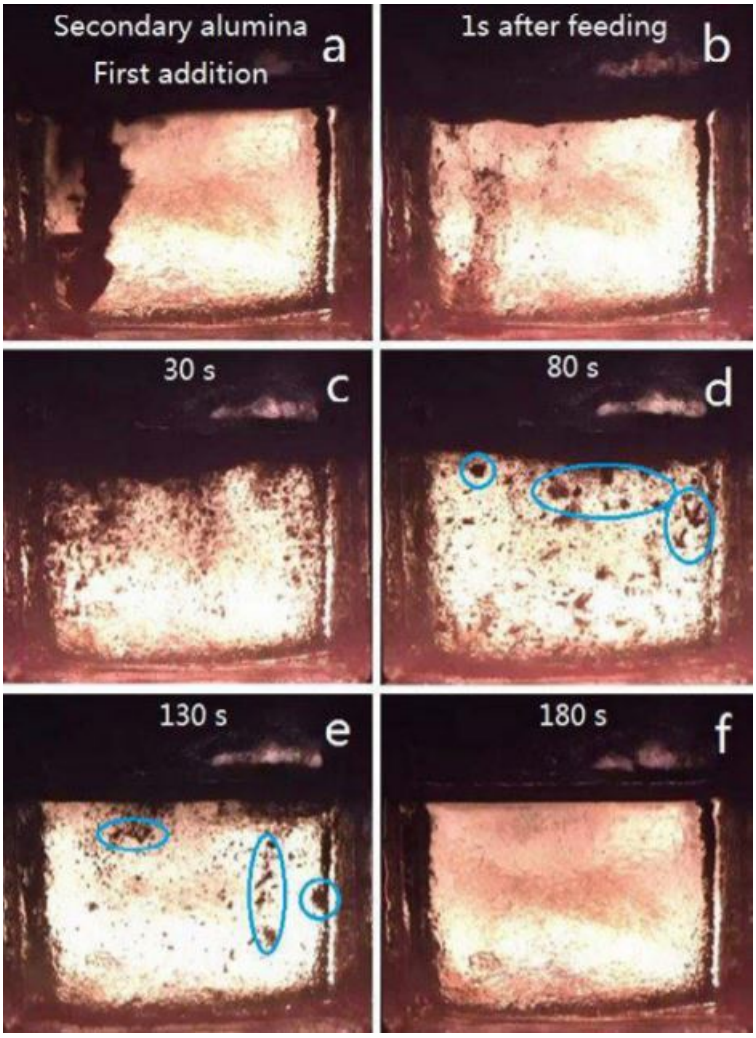

Figure 2.15: Dissolution of 2 grams of secondary alumina in cryolite, taken from [23]

Gao et al. [24] performed similar experiments as Yang et al. For the alumina dissolution experiments they used the side-view transparent cell from Figure 2.16. The bottom-view cell from Figure 2.16 was made to observe bubble behavior between the anode and cathode.

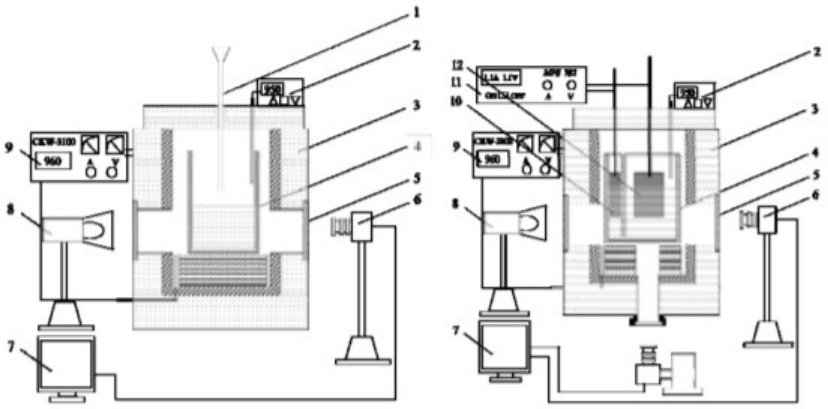

(a) Side-view transparent cell (b) Bottom-view transparent cell

The schematic diagrams of side-view transparent cell and bottom-view transparent cell: 1 – Charging pipe; 2 – Thermocouple; 3 – Furnace; 4 – Quartz Crucible; 5 – Side-view Quartz Window; 6 – High Speed Camera; 7 – Computer; 8 – Light Source; 9 – MPS 3100 Temperature Controller; 10 – Cathode; 11 – 702 DC Power Supply; 12 – Anode

Figure 2.16: Figure of the setup used by Gao et al.[24]. The side-view cell is based on the setup used by Haupin [22], while the bottom-view transparent cell was developed by Northeastern University Shenyang, China.

Gao et al. [24] observed similar behavior for the dissolution as Yang, with a sinking crust for primary alumina. However, no crust formation was observed for secondary alumina. The dissolution process for primary alumina took 600 seconds, while the process took 113 seconds for secondary alumina.

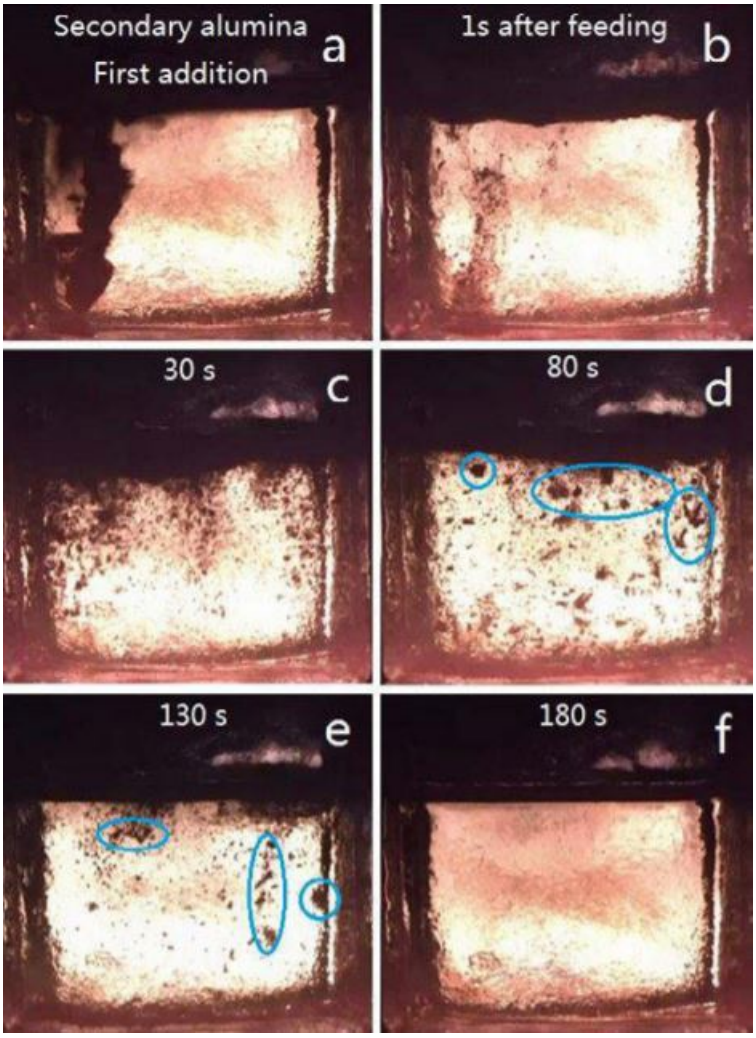

Figure 2.17: Dissolution of primary and secondary alumina respectively in cryolite at 955°C, taken from Gao et al. [24]

Aulie [18] performed dissolution experiments in a see through cell to find out the optimal setup for future experiments. Experiments conducted with pure synthetic cryolite was found to be non-ideal for experiments due to the high temperature needed for the bath to melt. This lead to destruction of crucibles before it could become transparent, as can be seen in Figure 2.18.

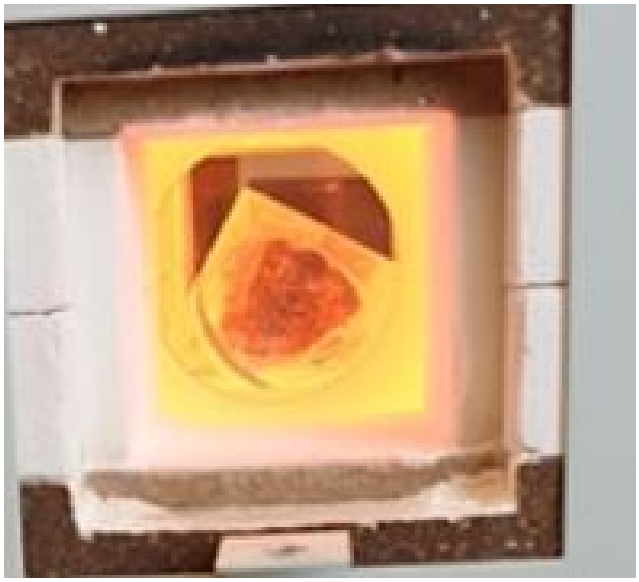

Figure 2.18: Picture of a destroyed crucible inside the see through furnace. The experiment were performed by Aulie [18] at 14.10.2019

After switching from synthetic cryolite to an industrial bath Aulie was able to get a successful dissolution experiment. It was concluded that a cryolite mixture more similar to industrial standards was needed in order to reduce the necessary temperature.

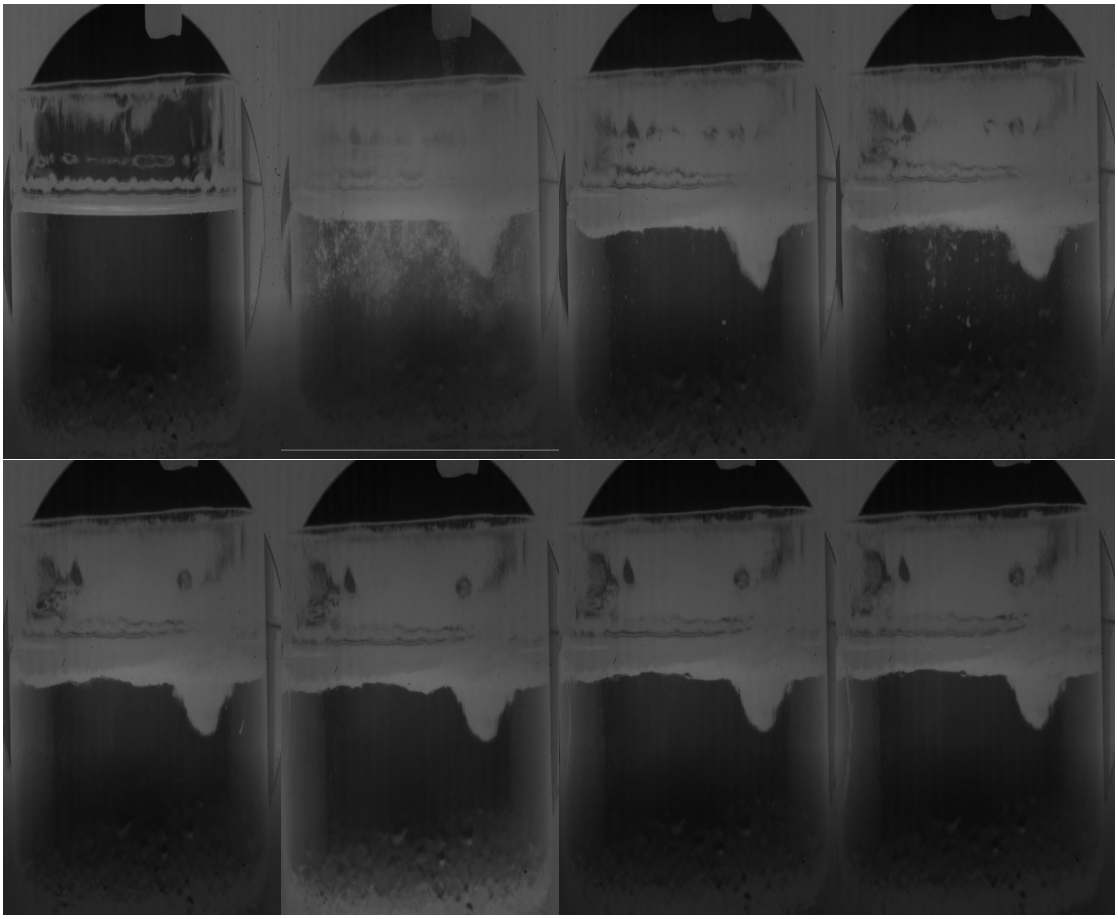

Figure 2.19: Dissolution of alumina in a see through cell. Pictures are from before addition, 5 seconds after addition, 30 seconds, 60 seconds, 120 seconds, 180 seconds, 240 seconds and 300 seconds respectively. The experiment was done on 20.11.2019 by Aulie [18].

Bracamonte et al. [25] performed dissolution experiments in a see-through cell shown in figure 2.20 to examine the use of an Alumina sensor for emf measurements as a method of determining alumina concentration in cryolite melts. The measurements from the sensor was in agreement with the observations done in the see through cell, making it a potentially valuable tool in dissolution experiments for closed cells as well where visual observations is not possible. Bracamonte examined dissolution for primary and secondary alumina and analysis of particle size distribution and surface morphology for the two alumina types. Secondary alumina was found to dissolve much faster, which was in accordance with the data from the analysis.

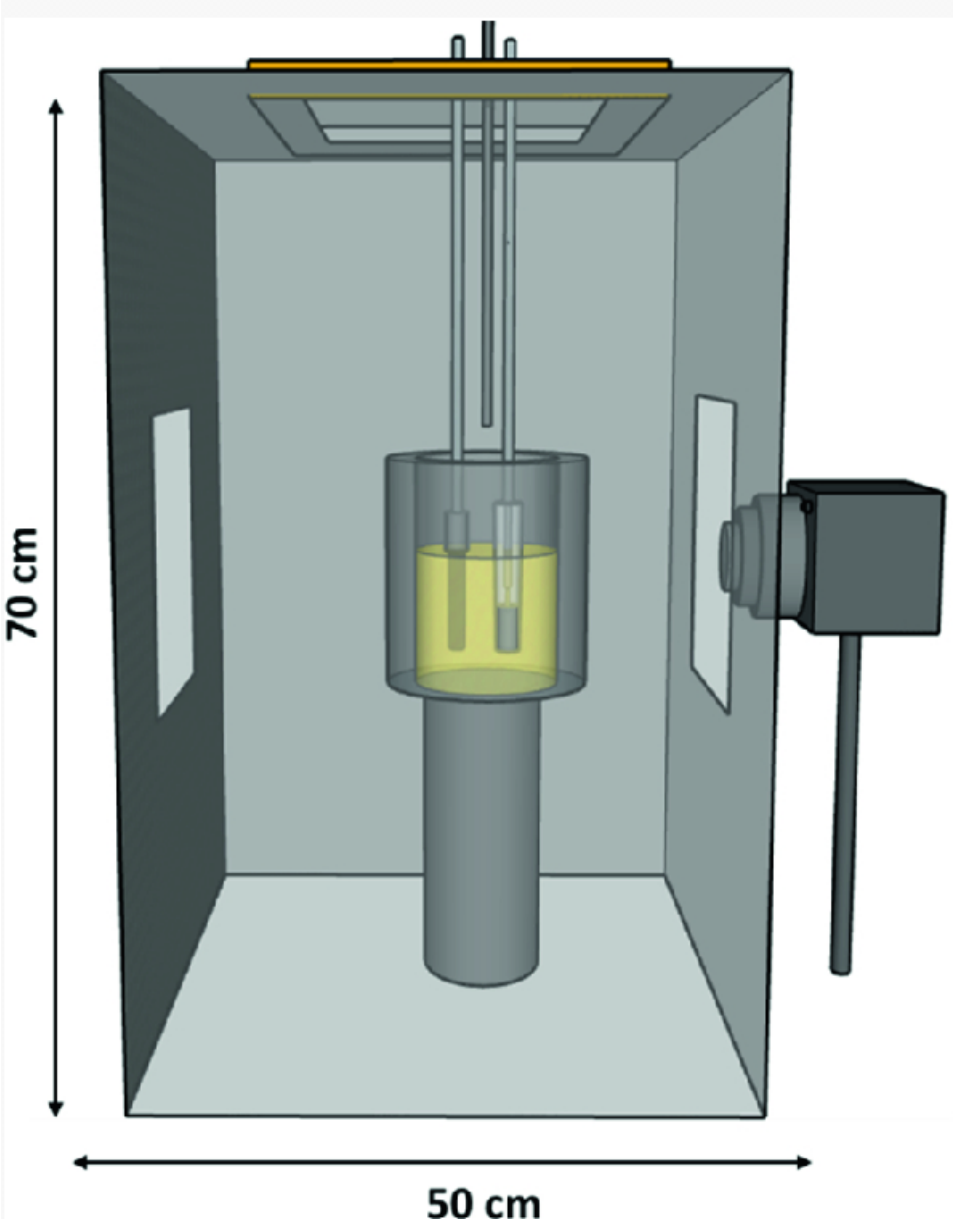

Figure 2.20: Schematic of the setup of the see through oven used by Bracamonte [25]

3 Experimental

3.1 Setup

The see through cell used in the Master's project consists of an Entech vertical tube furnace constructed with two 10x10 cm holes on each side of the oven equipped with shutters with mounted windows. The furnace can be heated to 1200°C. The furnace is designed with a 15 cm open space inside. Quartz-crucibles of 7.5x6.5 cm height and width are used in the experiments. All experiments were filmed with a Photron Mini Ax high-speed camera from one side and a Sony camera from the other side. Figures 3.1 shows the furnace from one side with the shutters on. The furnace is placed under fume extractors and are cooled down with running water.

Figure 3.1: Picture of the furnace used in the experiments.

The two holes on the side of the oven is placed approximately 18 cm above the bottom of the furnace. A 'tower' consisting of smaller parts like tubes and discs was made so the quartz crucible would be placed along the holes. The bottom of

the tower were always a crucible to protect the bottom of the oven from damage in case of a failed experiment with a broken crucible. To protect the oven from possible splashes from the cryolite a Pythagoras tube with holes similar to the ones on the oven was placed inside the furnace. Several radiation shields was attached to the lid of the oven. Figure 3.2 shows a picture of the furnace with both shutters taken out and a crucible filled with water inside.

Figure 3.2: Picture of the see through cell with both shutters open and a crucible filled with water inside.

Melt experiments were done by adding cryolite mixture to the crucible, placing the crucible in the furnace and heating it up to 940°C and then increasing the temperature until the bath had melted and the crucible were transparent. The oven was purged with nitrogen to get as neutral environment inside the oven as possible. Once the cryolite had melted and the crucible was transparent The feeding tube was then opened and approximately 1 wt% of alumina was fed to the melt.

3.2 Cryolite mixture

As was concluded in the project work [18] pure synthetic cryolite was not desirable to use as a bath due to high melting temperature. Industrial baths are also not ideal because it is necessary to have a similar bath for each experiment to get comparable results. Finding the exact composition of a bath from the industry is not an easy task, so using an industrial bath for the experiments would require one large batch from the same supplier. Instead it was decided to attempt creating a bath with similar characteristics as one from the industry.

A base of synthetic cryolite was tried out as the cryolite mixture. To lower the melting temperature aluminium fluoride (AlF_3), calcium fluoride (CaF_2) and primary aluminium oxide (Al_2O_3) was chosen as additives. To ensure that the bath would not contain any unwanted additives the aluminium fluoride went through sublimation treatment before being used as an additive. The primary aluminium oxide was provided by Alcoa and the entire batch was taken from their plant in Mosjøen the same day. To simulate industrial standards described by Grjotheim et. al [1] a composition of synthetic cryolite with 15% excess AlF_3, 6% CaF_2 and 2% Al_2O_3 was tried out.

Due to issues with a high smelting temperature for the cryolite mixture a bath made up of industrial bath and excess lithium fluoride (LiF) was used to lower the smelting temperature further. The bath was made by weighing out crushed industrial bath and LiF separately and mixing them together in a closed container before transferring the bath to the crucible used for the experiment.

3.3 Materials

The data in Figure 3.1 was given for the primary alumina before it went through the dry scrubbers at the plant, so values for the secondary alumina might be slightly changed.

Table 3.1: Physical data for the main alumina used in this work given by the producer

Parameter	Unit	Value
Surface area	m^2/g	72.4
LOI	%	0.58
Moisture	%	0.15
Gibbsite	%	0.1
- 20 microns	%	0.7
+ 100 mesh	%	8.2
+ 325 mesh	%	92
Attrition index	%	11

The industrial bath used in the experiments was provided by Sintef, and the exact contents are not available. The initial amount of Al_2O_3 was estimated around 2%. Excess lithium fluoride (LiF) with 98% purity was added to the industrial bath.

3.4 Initial Experiments

The initial experiments was completed by the author outside of the current time for the Master's project. The experiments shown shows the differences between primary and secondary dissolution of alumina. The experiments was done with a different cryolite mixture, one based on synthetic cryolite instead of industrial cryolite. They are not counted in the experiments conducted for this project.

3.5 Experiments conducted

3.5.1 Establishing a standard

By controlling the bath composition an attempt to make a standard for the dissolution experiments was done by comparing them to to each other. Since the same bath was used for every experiment dissolution times should be the same within statistical significance. This was done to create a baseline for dissolution times with no extra additions in either the bath or alumina, which can be used to examine the effect of changes to the standard experiments.

3.5.2 Sulfur

Possible influence of sulfur on dissolution of alumina in cryolite was examined by mixing sodium sulfate (Na_2SO_4) with the alumina being fed to the cell. Sodium

sulfate was weighed out and mixed with alumina by adding both powders to a closed container and mixing them together. The amount of sodium sulfate added varied for the different experiments, from 2 to 10 wt%. The exact amount is mentioned in table 4.2. One experiment was done with 20 wt% sodium sulfate due to a calculation error.

3.5.3 Carbon

Possible influence of carbon on dissolution of alumina in cryolite was examined by mixing carbon into the industrial bath. The The carbon was crushed and sieved with a 100 μ m sieve to get rid of the larger carbon particles. The carbon used in this project was industrial coke delivered from Hydro Aluminium. The amount of carbon used each experiment is mentioned in table 4.3.

3.5.4 Table of the experiments conducted

Table 3.2: Table presenting all the melt experiments done during the Master's project.

Date	**Experiment type**	**Feed**	**Comment**
14.04	Establishing a standard	2	Different bath composition from other experiments, 3% excess LiF
16.04	Establishing a standard	4	Different bath composition from other experiments, 4% excess LiF
20.04	Sulfur	4	Problems with the high-speed camera - could not save videos
22.04	Sulfur	4	Third addition was without sulfur
26.05	Carbon	4	Unclear window on the side of the high-speed camera
28.05	Carbon	4	
01.06	Carbon	4	
03.06	Sulfur	4	

3.6 Image processing

The videos taken during the experiments were converted to a sequence of images with a program called Free Video to JPG converter. The image stack was then opened in ImageJ and the image was cropped to only contain the crucible, and then cropped again to only get rid of the parts of the crucible that would only contribute to background noice. To perform treshold analysis the color of the raft had to be distinguishable from the crucible, which was often not possible for the

sides and bottom of the crucible. The area below the surface was then chosen for further analysis, as shown in figure 3.3.

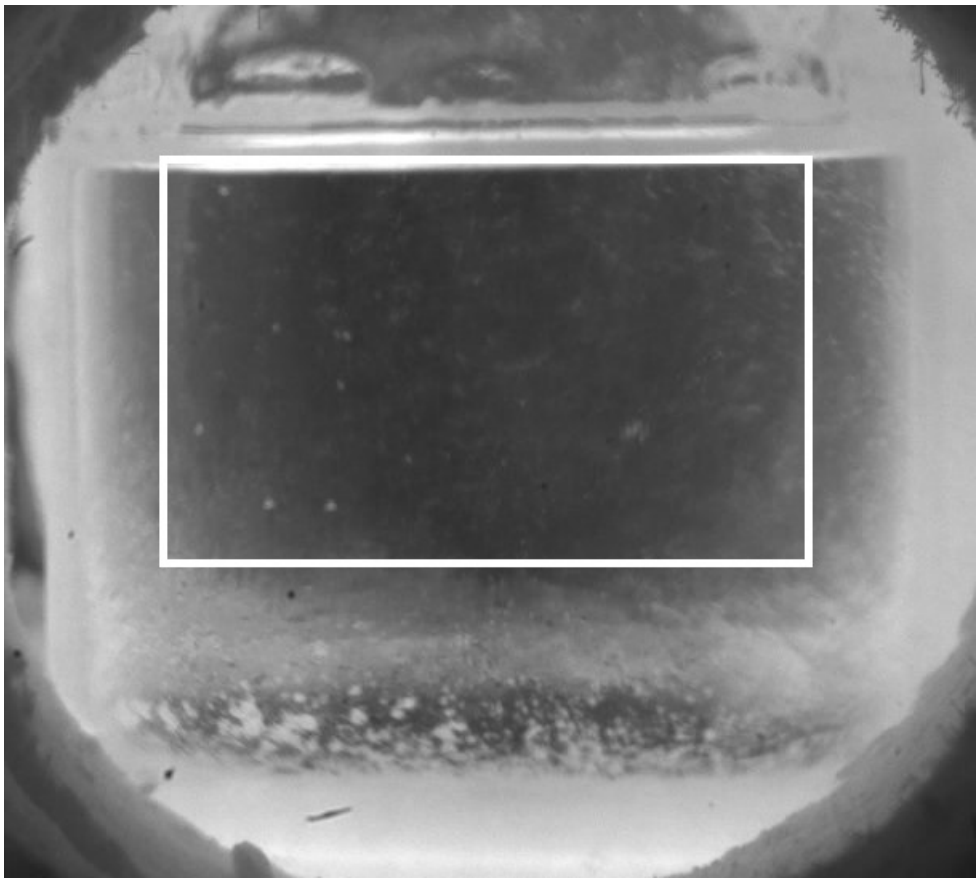

Figure 3.3: Example of cropping area

Treshold analysis is an analysis where you remove color from a picture to be left with only grey colors, and then add color to parts of the image. Once an area was chosen as described the brightness and contrast of the image was changed to further distinguish between raft and cryolite while trying to keep the background noises as low as possible. Then treshold was applied and ideally only the raft would get colored. As is shown in figure 3.4 some background noise had to be colored as well.

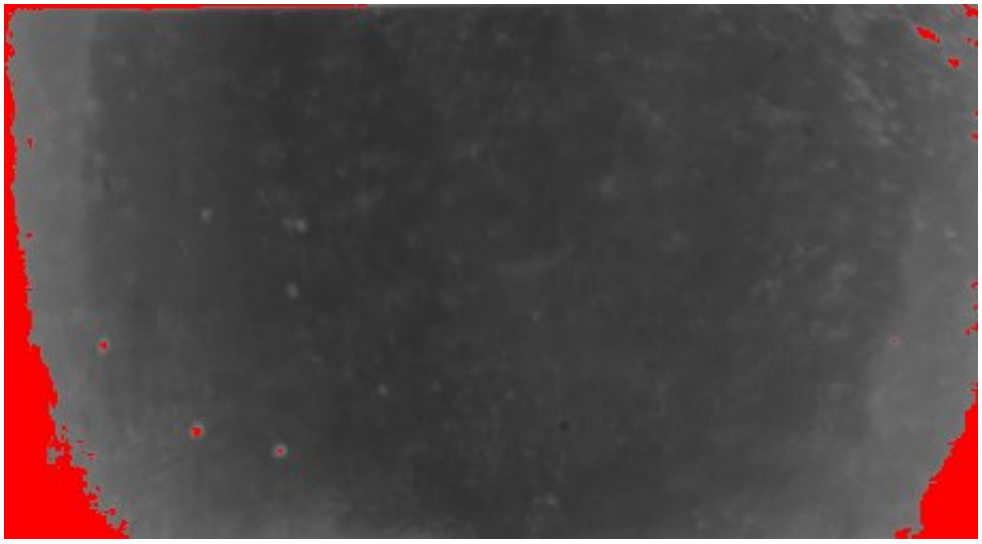

Figure 3.4: Exampe of treshold appliance.

With treshold applied to the entire image stack a script was set to run. This script looks at every image and gives out a percentage of how big a part of the image was colored. This percentage can then be plotted against time to show the dissolution process.

The plan for the project was to use both videos from the high speed camera and the sony camera for the image processing in ImageJ. The method worked well with the high speed camera, but issues with reflections and fumes for the sony camera made it impossible to do any analysis. Only videos from the high speed camera were examined with this method, and a selection of them are presented in the results part. The images showing the dissolution are compressed to make each figure fit into one page.

3.7 Dissolution times

Since ImageJ could not be utilized on the entire dissolution process, dissolution times had to be decided by looking at the videos from the sony camera and deciding when the dissolution was done. The criteria for the dissolution process to be done was chosen to be when the area under the surface was empty, i.e when all the alumina has sunk to the bottom of the crucible.

4 Results

4.1 Initial experiments

4.1.1 Dissolution of Primary Alumina

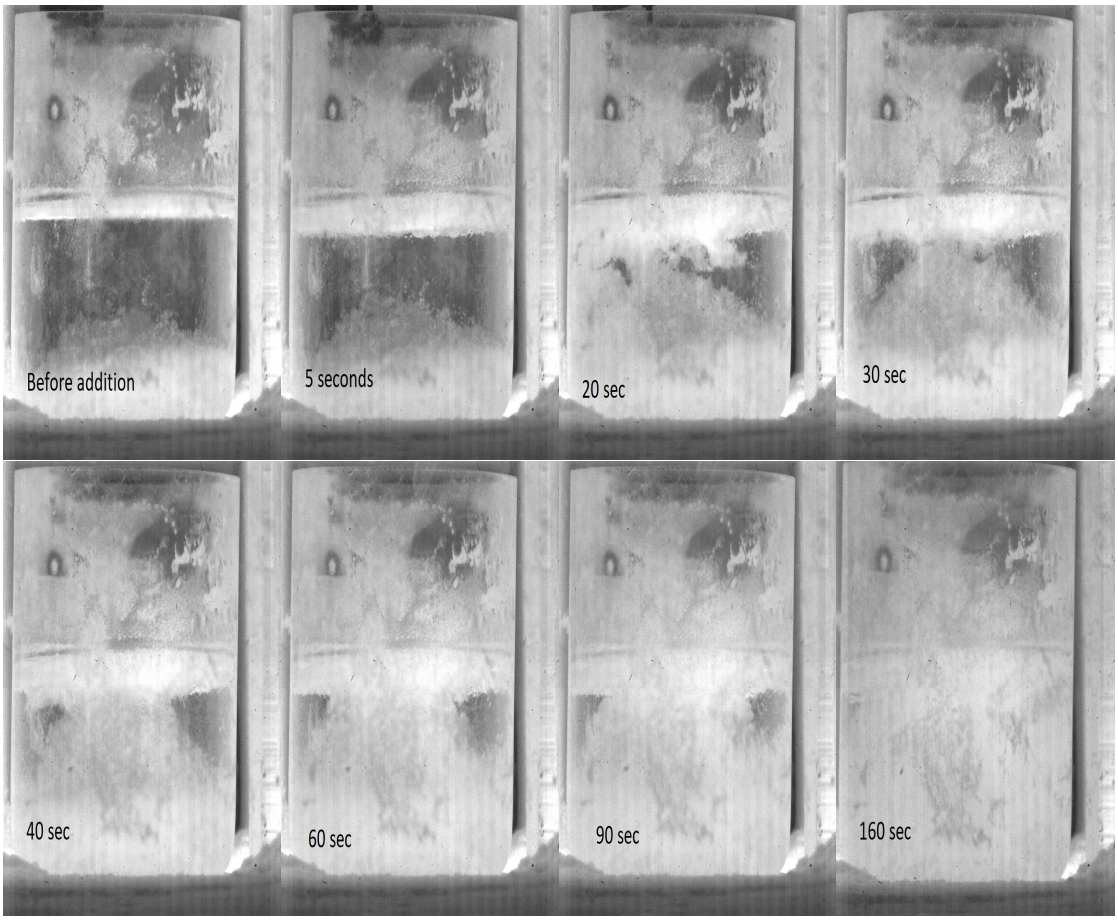

Figure 4.1: Pictures from feeding of primary alumina done on 02.06.2020. Video available at `https://youtu.be/fLMrKcVCH4A`

4.1.2 Dissolution of Secondary Alumina

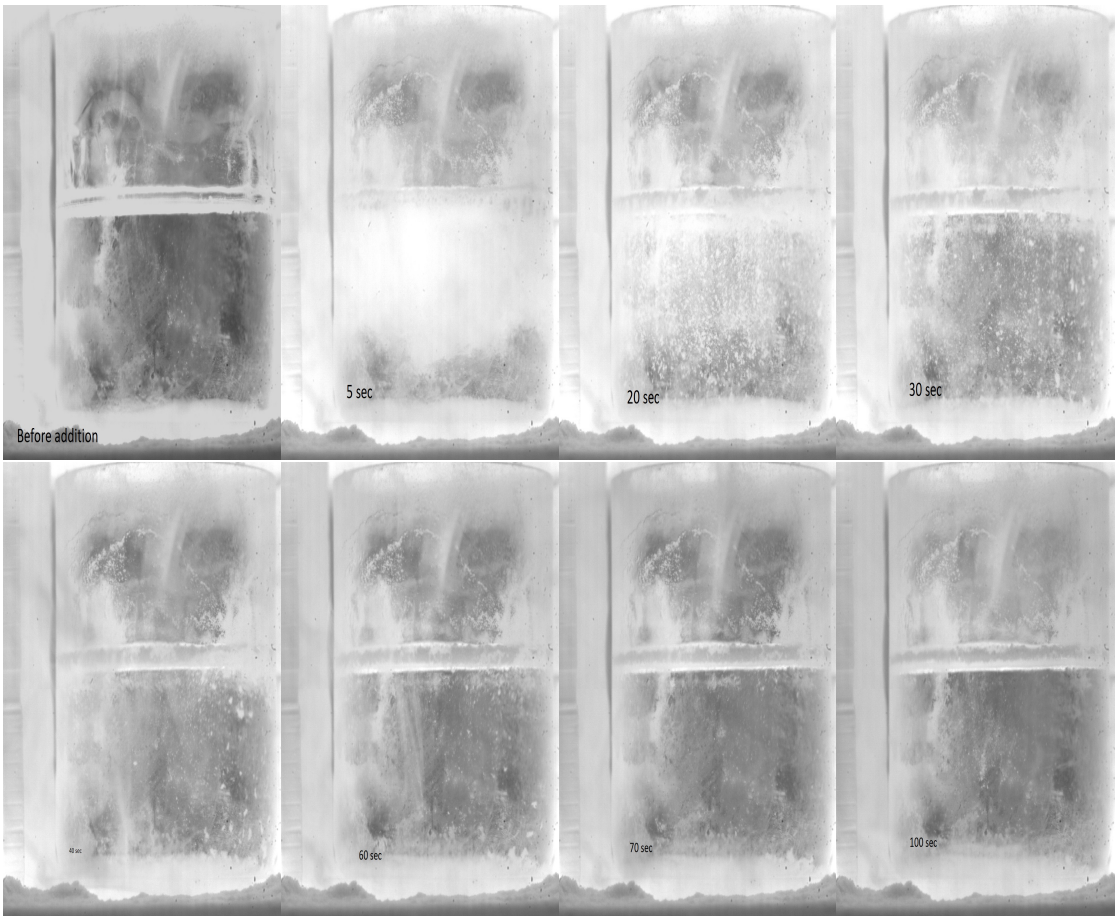

Figure 4.2: Pictures from feeding of secondary alumina done on 12.05.2020. Video available at `https://youtu.be/LEzejFKUhF8`

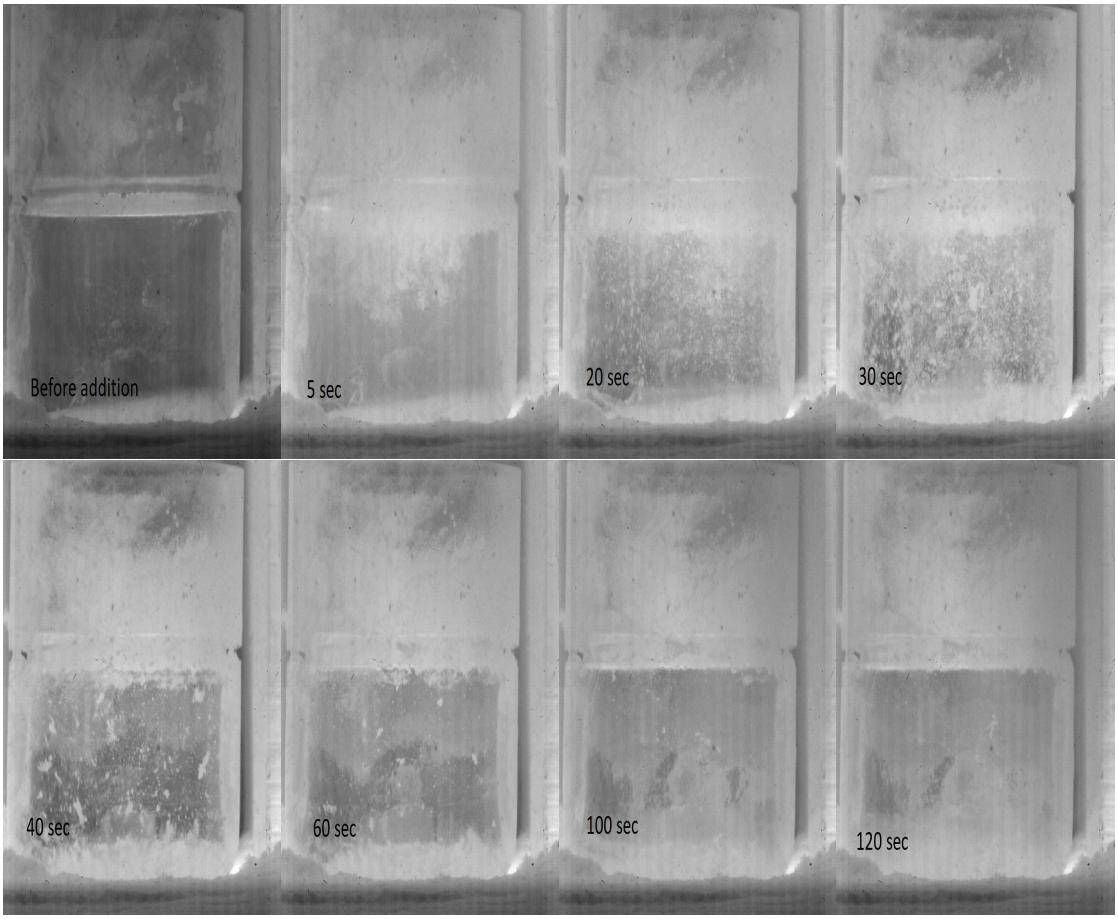

Figure 4.3: Pictures from feeding of secondary alumina done on 02.06.2020. Video available at `https://youtu.be/HiIT-CYDToY`

4.2 Establishing a standard

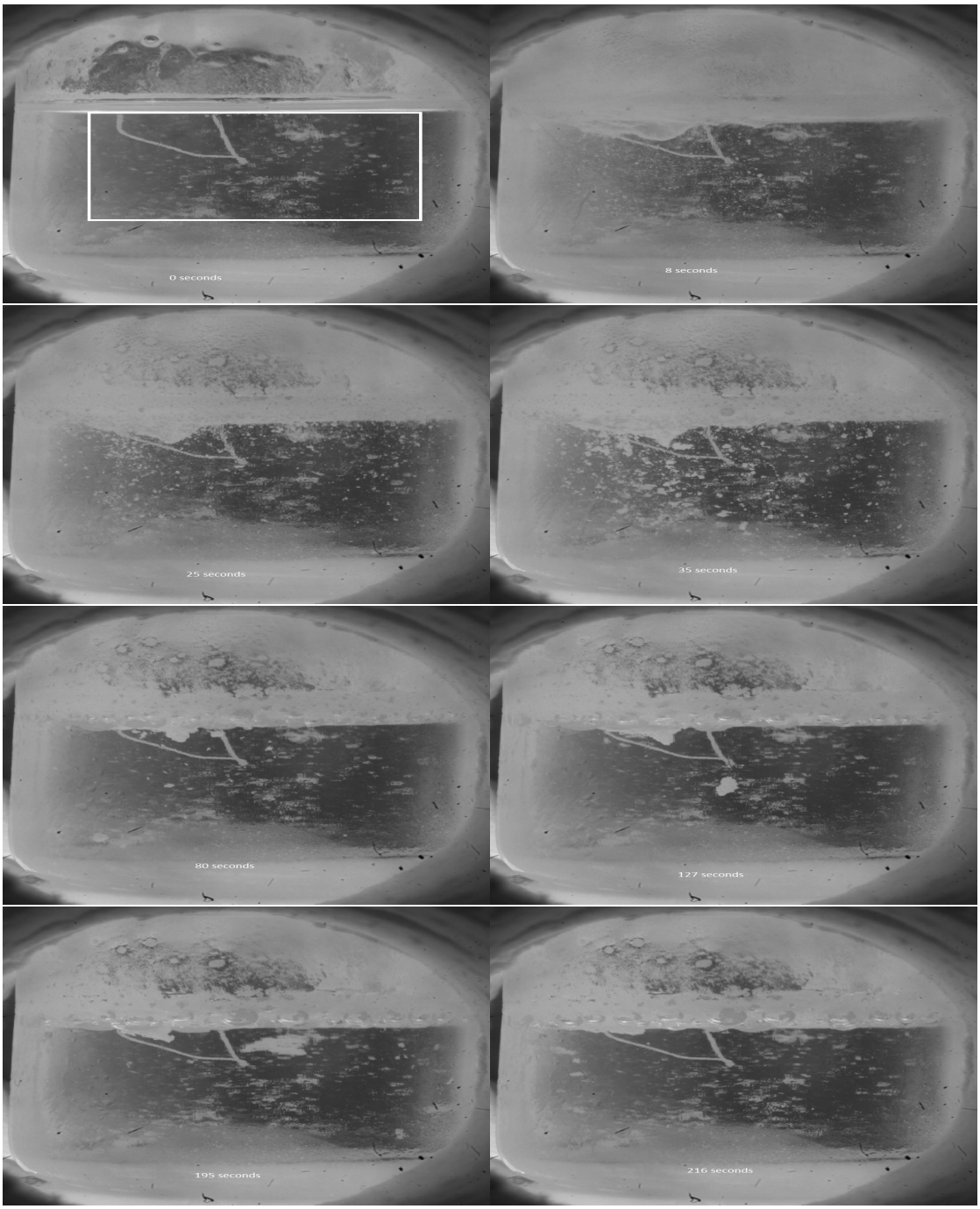

Figure 4.4: Pictures from first addition of secondary alumina done on 14.04.2021. Video available at `https://youtu.be/MRvbWEhwCOA`

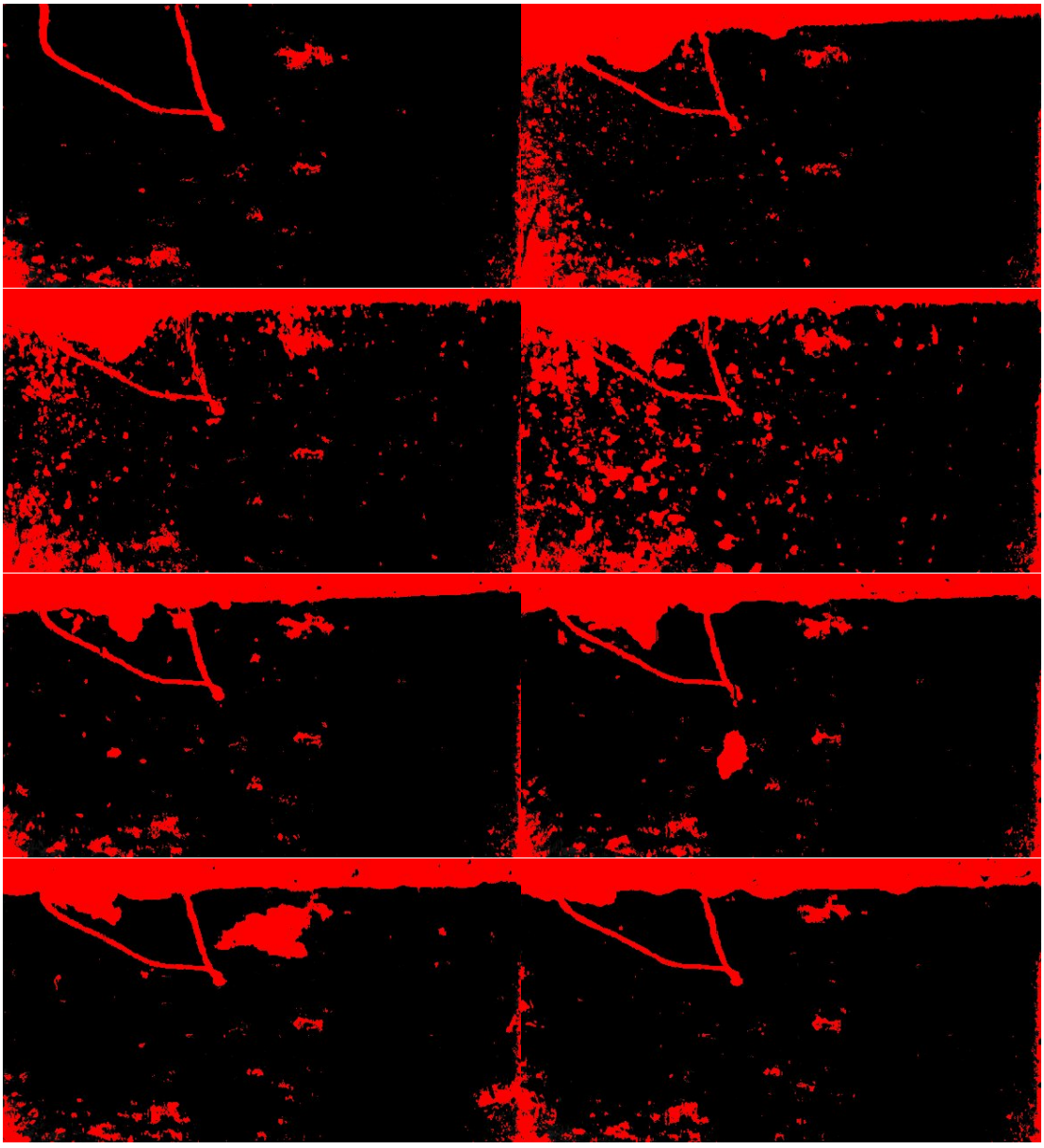

Figure 4.5: Figure 4.4 with applied treshold on area marked in first picture

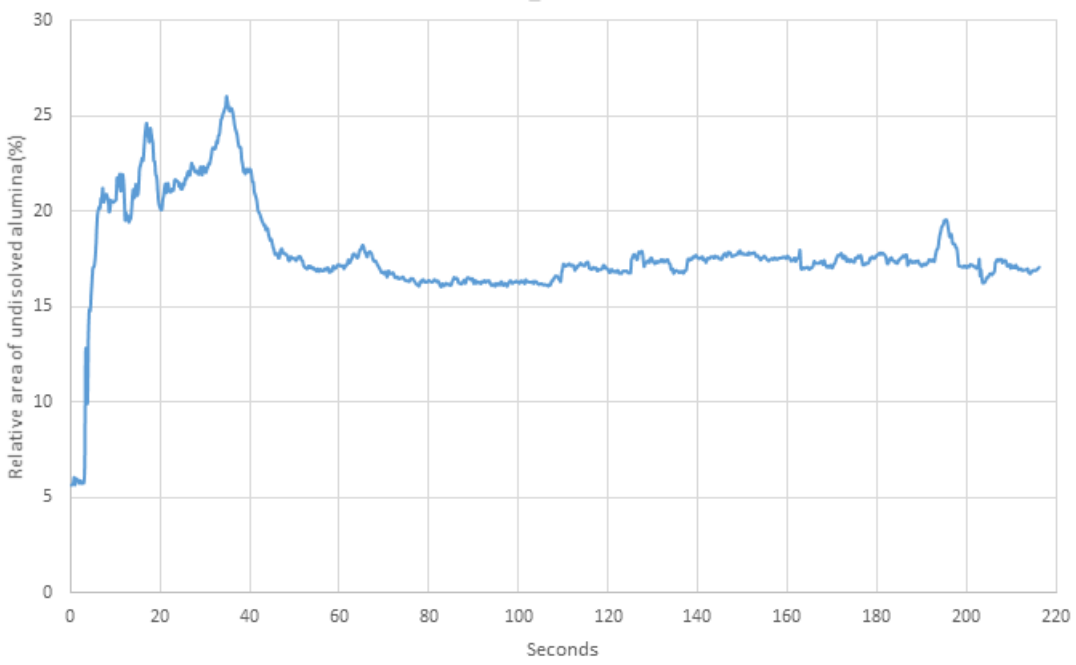

Figure 4.6: Graph showing the dissolution based on the treshold from figure 4.5

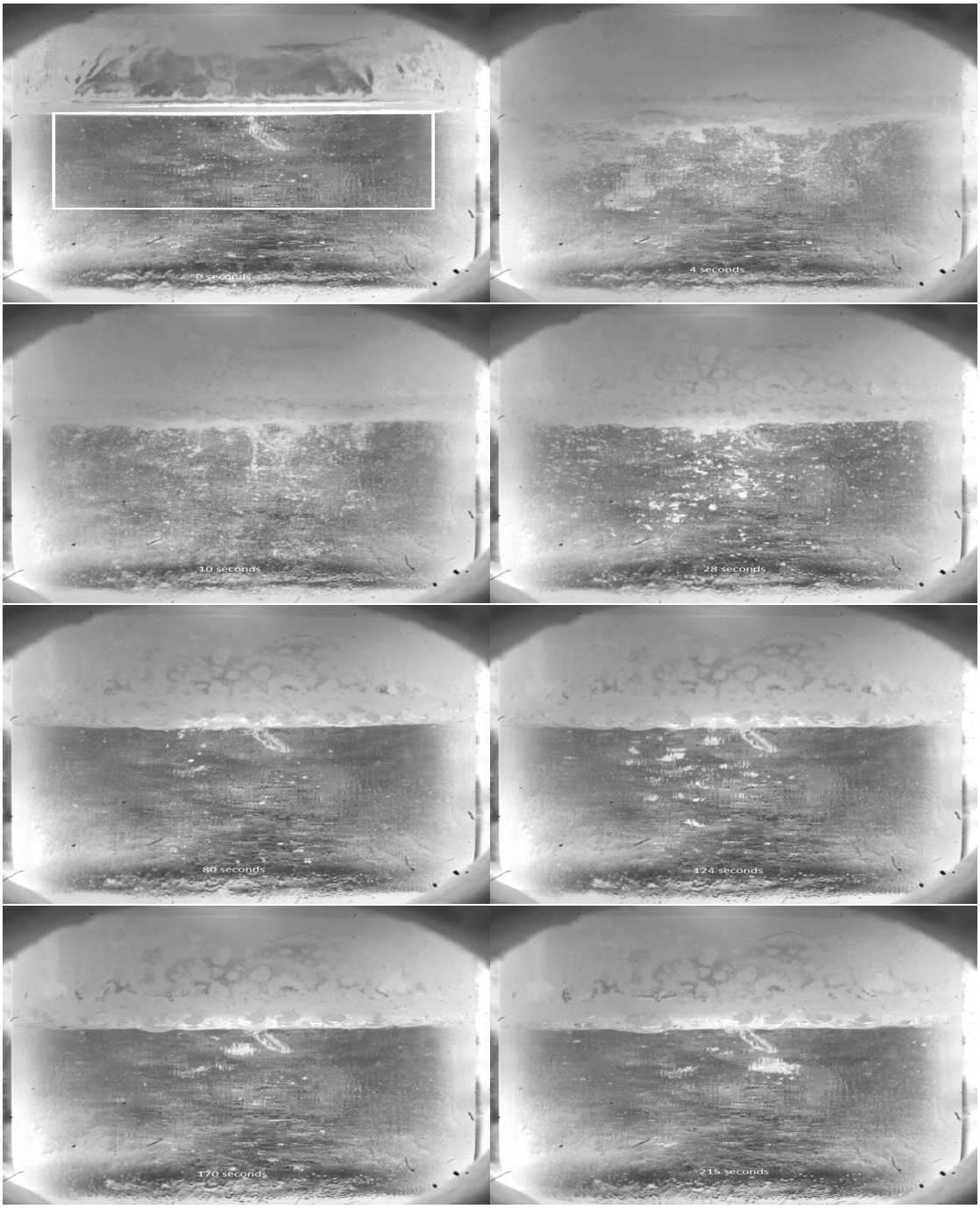

Figure 4.7: Pictures from first addition of secondary alumina done on 16.04.2021. Video available at `https://https://youtu.be/a6PzDtfYTHk`

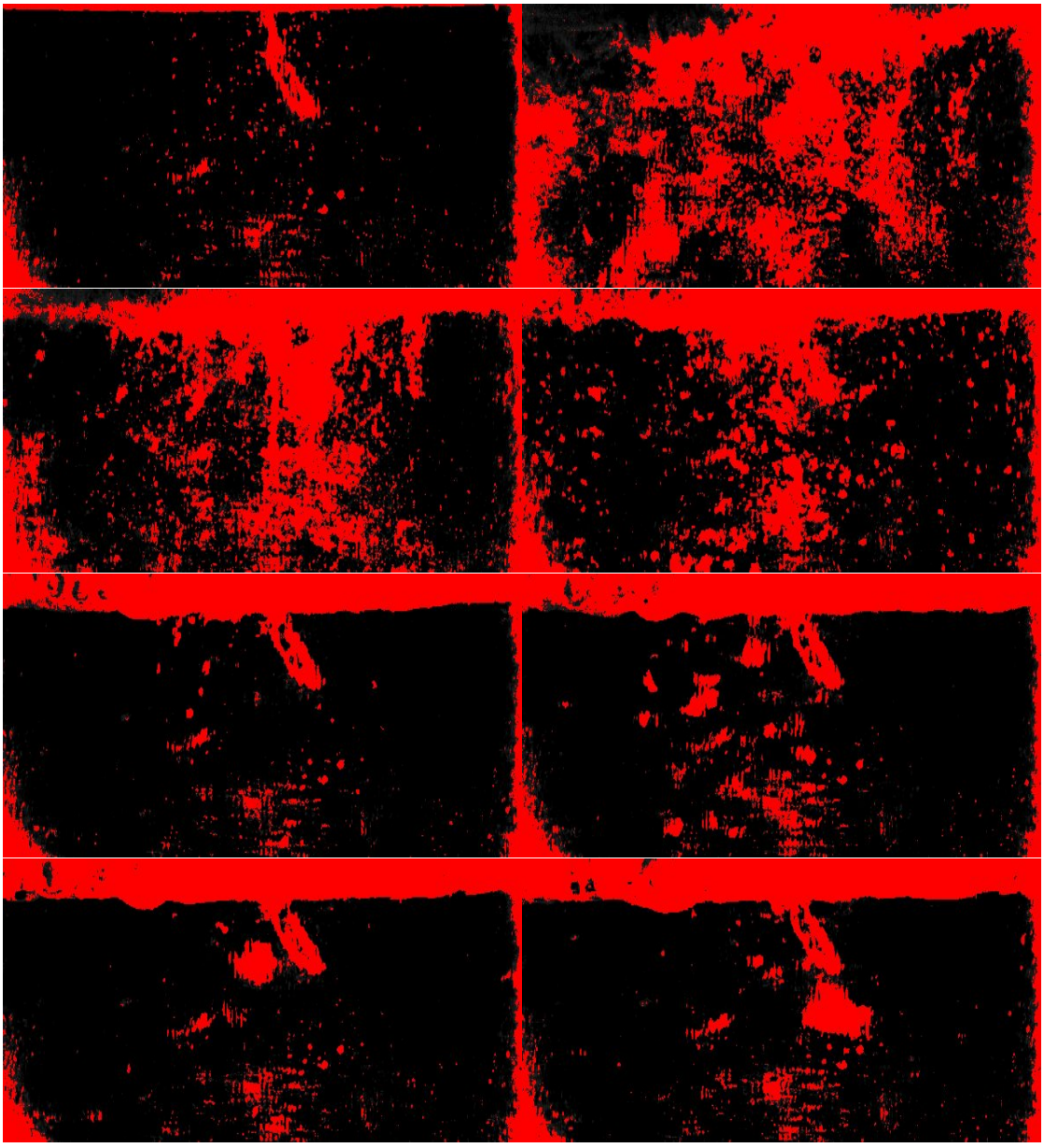

Figure 4.8: Figure 4.7 with applied treshold on area marked in first picture

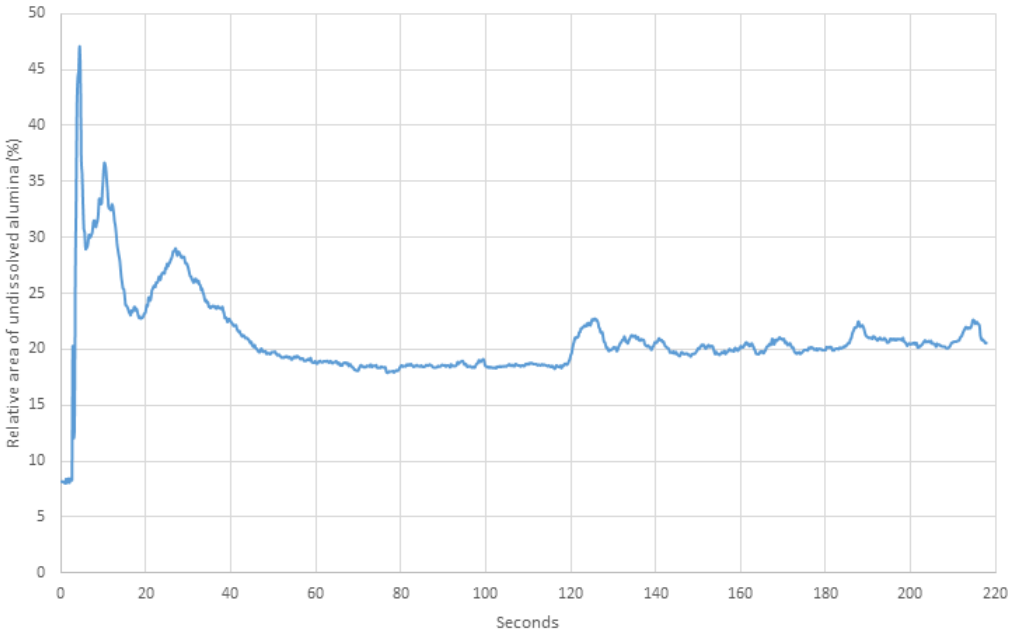

Figure 4.9: Graph showing the dissolution based on the treshold from figure 4.8

4.3 Sulfur

The experiment on 20.04 had problems with the high speed camera, so automatic processing was not possible for the additions this day.

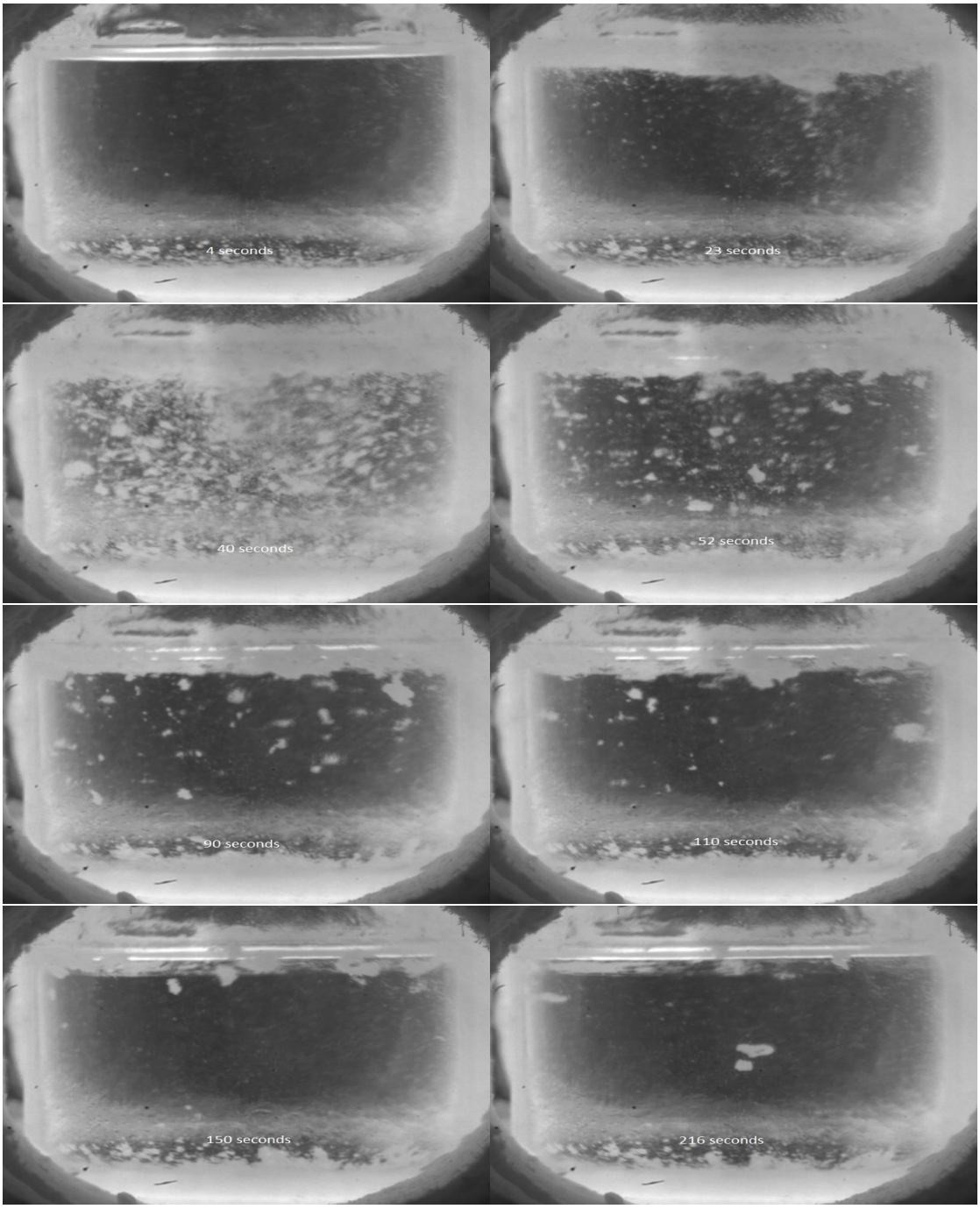

Figure 4.10: Pictures from first addition of secondary alumina with sulfur done on 22.04.2021. Video available at `https://youtu.be/5ExxSL3ZYww`

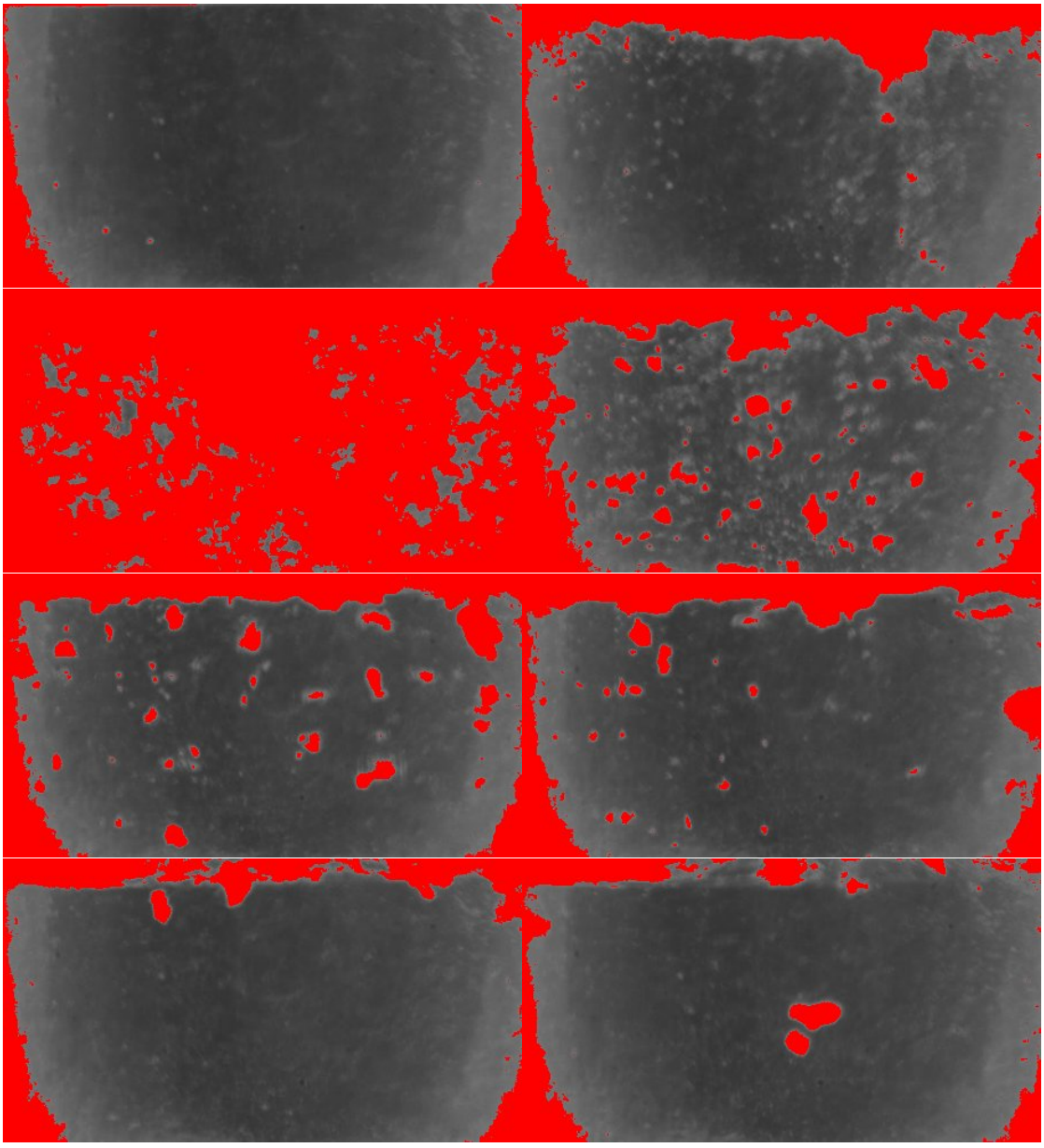

Figure 4.11: Figure 4.10 with applied treshold on area marked in first picture

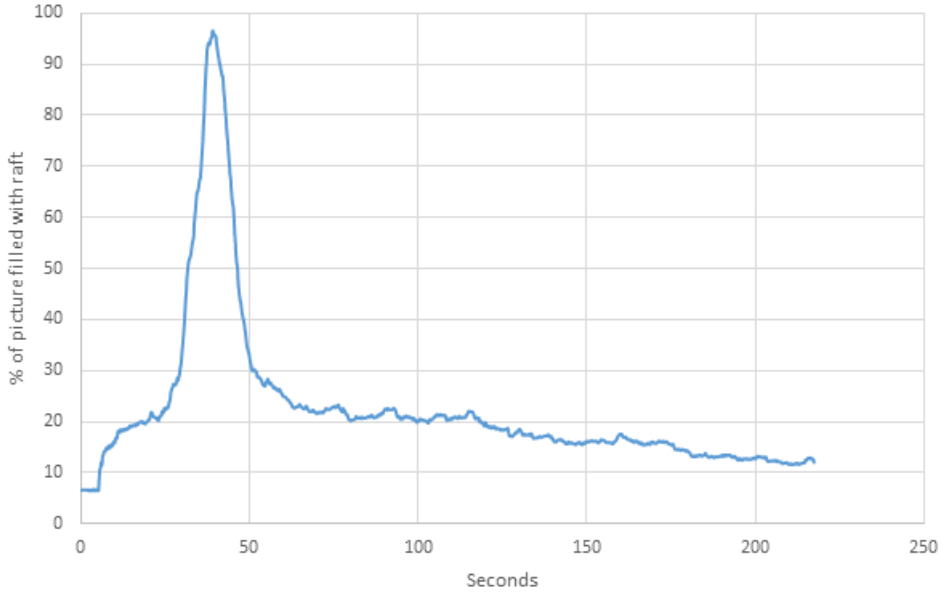

Figure 4.12: Graph showing the dissolution for first addition experiment at 22.04

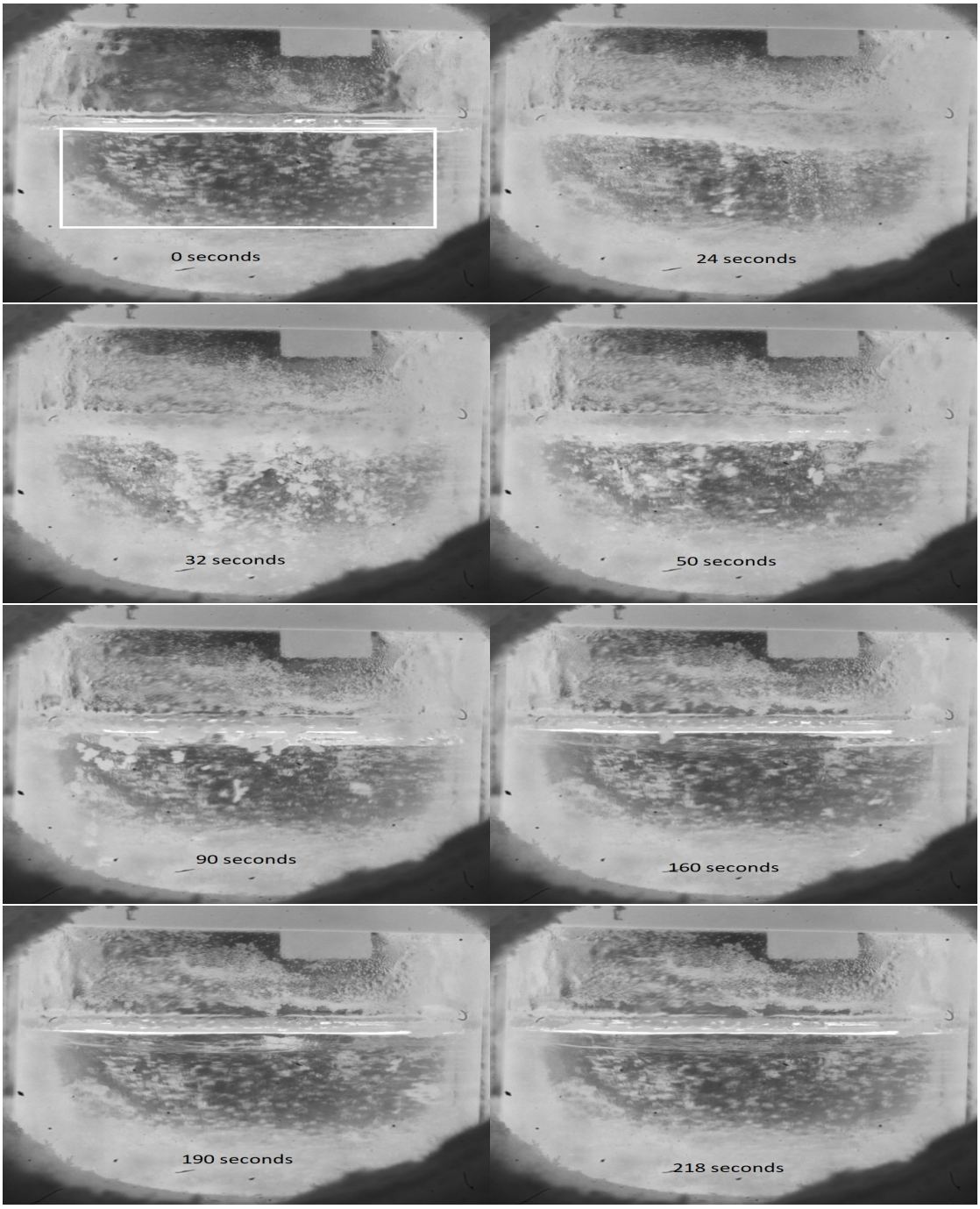

Figure 4.13: Pictures from second addition of secondary alumina with 4 wt% sulphur done on 03.06.2021. Video available at `https://youtu.be/TiS816L8f0s`

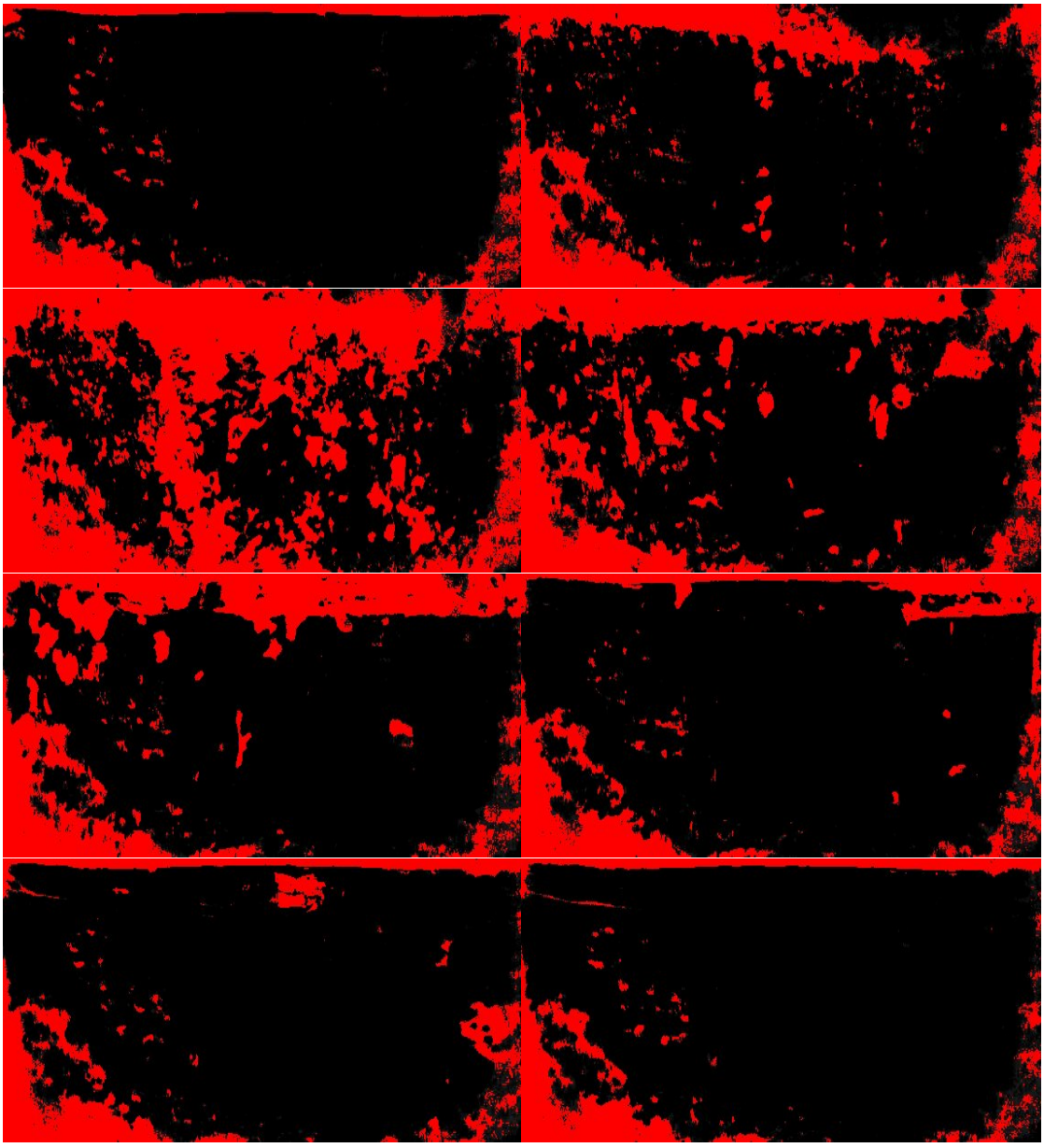

Figure 4.14: Figure 4.13 with applied treshold on area marked in first picture

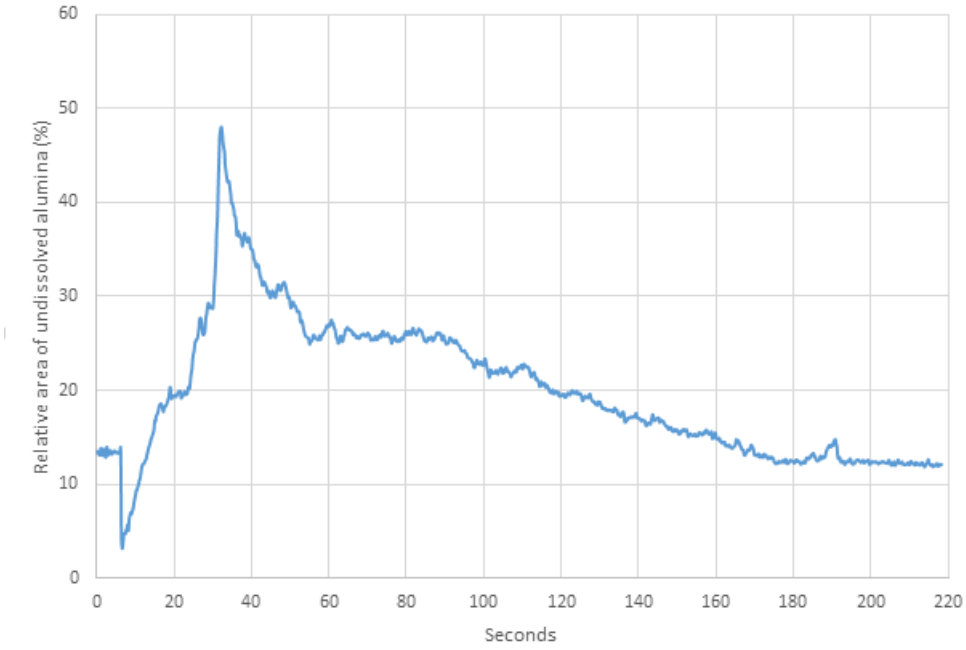

Figure 4.15: Graph showing the dissolution based on the treshold from 4.14

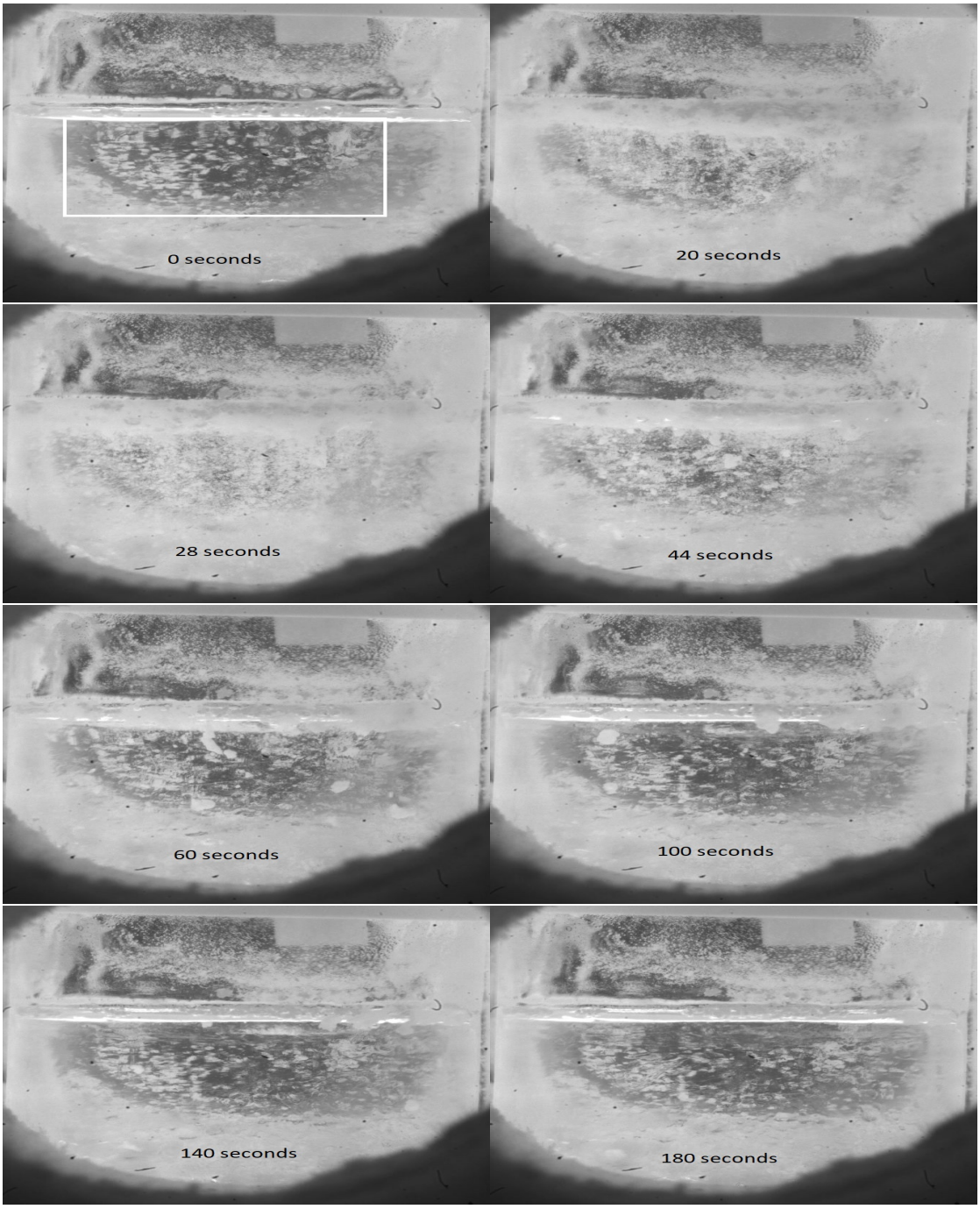

Figure 4.16: Pictures from fourth addition of secondary alumina with 4 wt% sulfur done on 03.06.2021. Video available at `https://youtu.be/MgkOwwfYHPI`

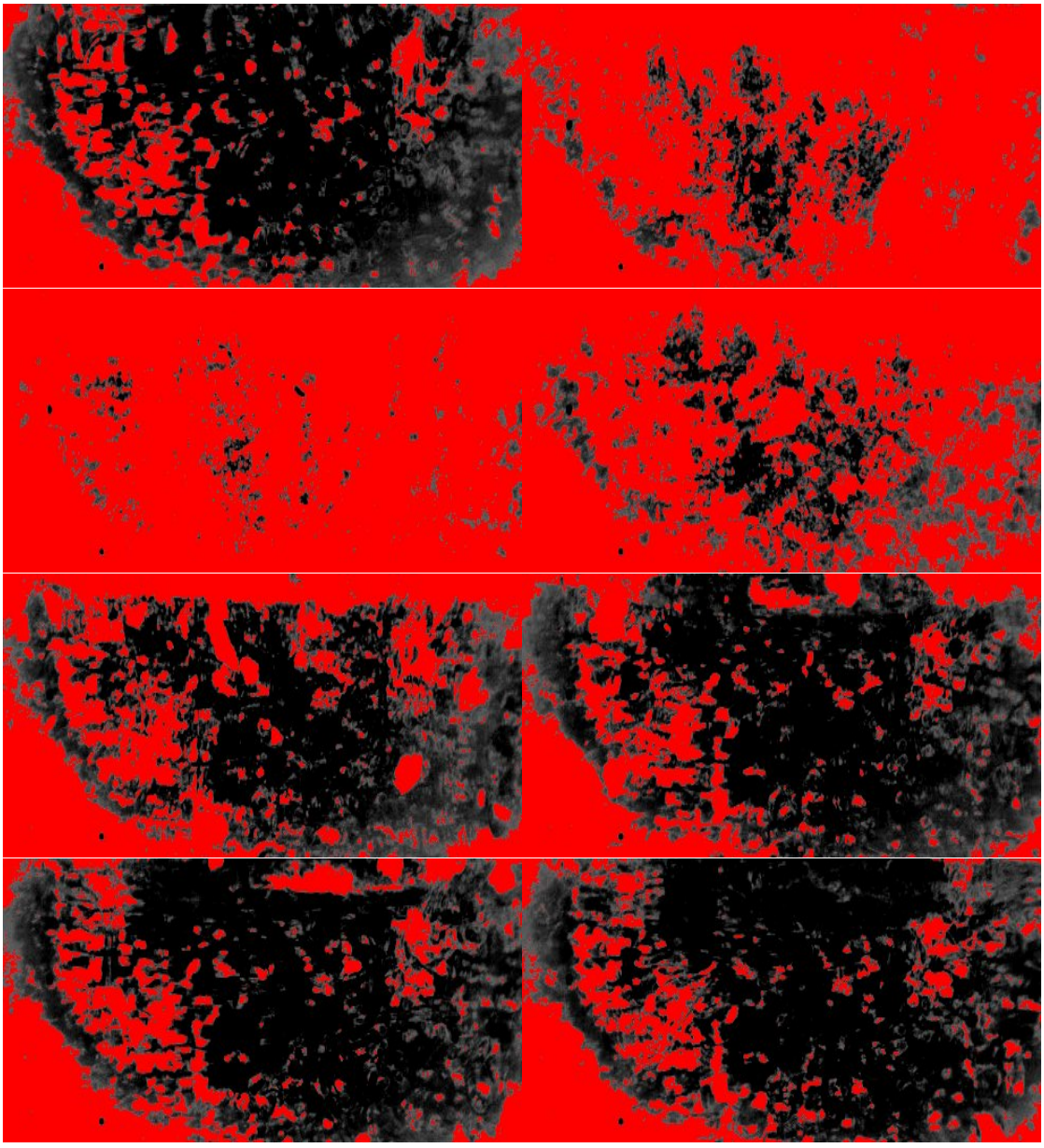

Figure 4.17: Figure 4.16 with applied treshold on area marked in first picture

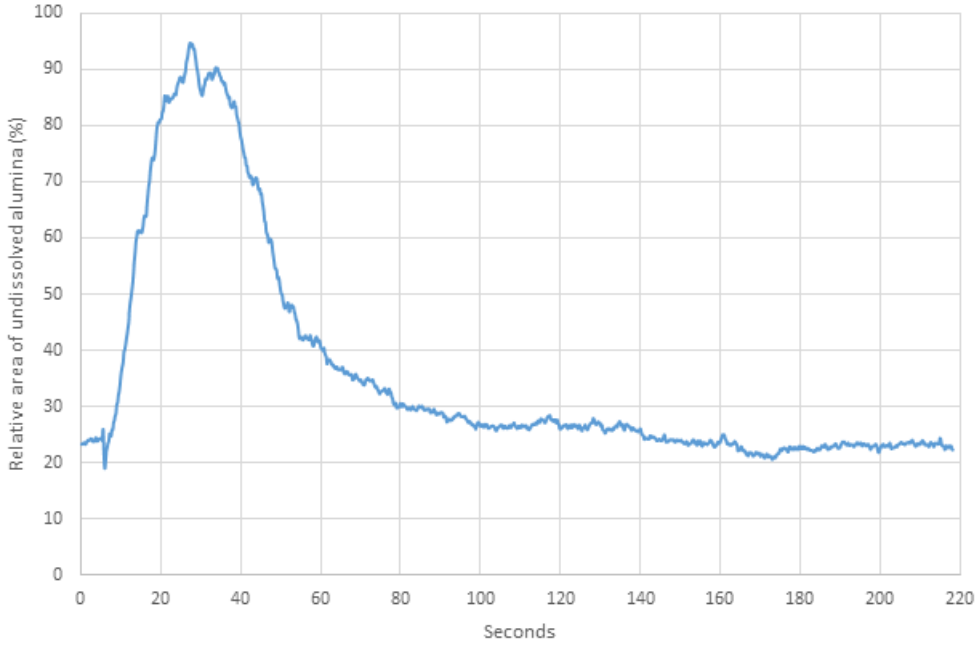

Figure 4.18: Graph showing the dissolution based on the treshold from 4.17

4.4 Carbon

The experiment at 26.05.21 with 1 wt% carbon in the melt had visual issues due to the window on the side of the high-speed camera getting a burn mark during heating of the oven. Figure 4.19 shows an image taken by the high speed camera, due to the black marks in the dissolution area treshold could not be applied on the raft. The video from the first addition this day can be found at `https://youtu.be/wW0n3vE69Ec`.

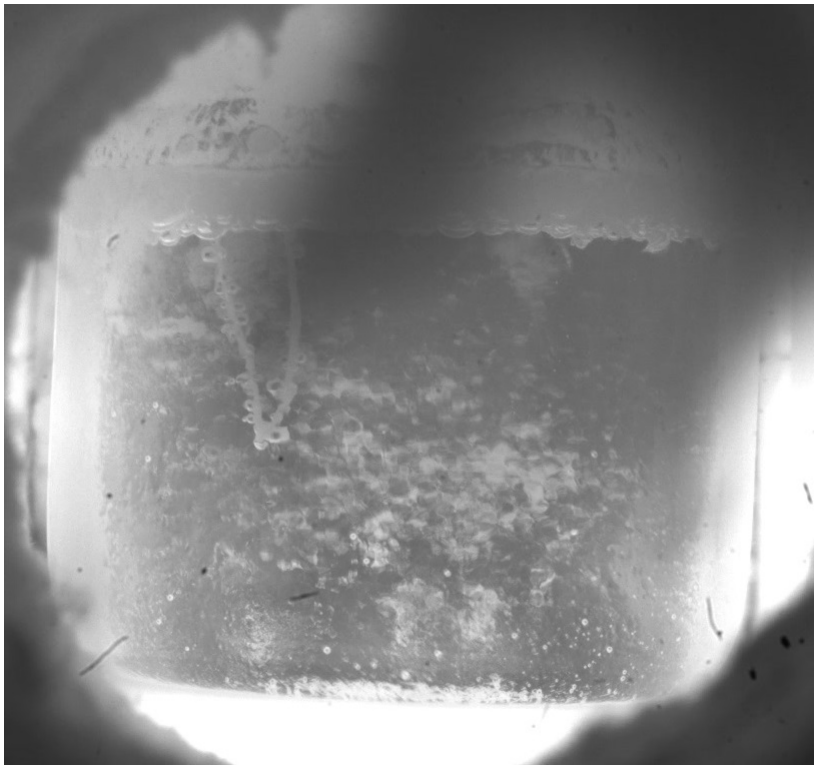

Figure 4.19: Picture showing the crucible at 26.05.21

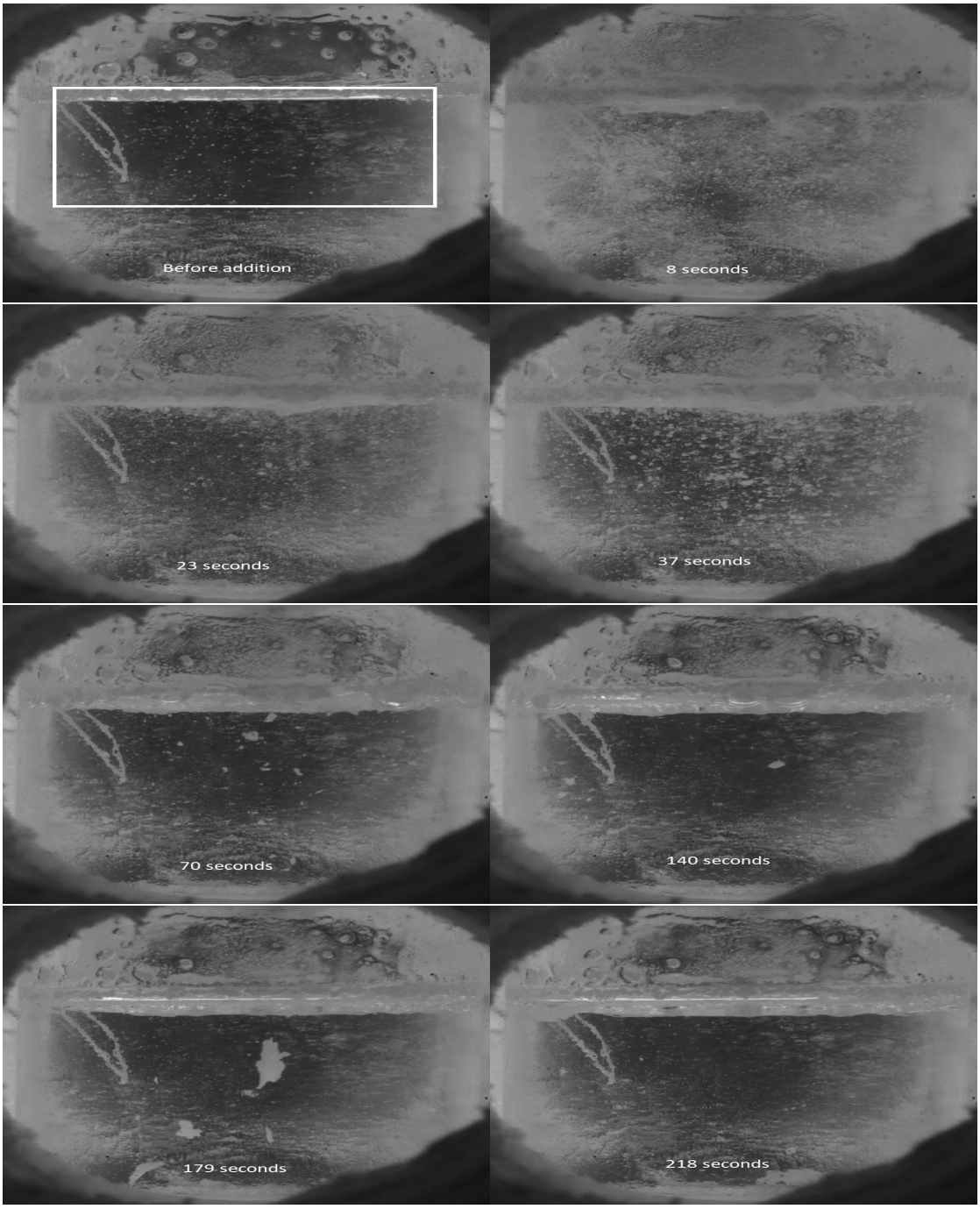

Figure 4.20: Pictures from first addition of secondary alumina with 0.1 wt% carbon in the bath done on 28.05.2021. Video available at `https://youtu.be/gnz5PlXdsso`

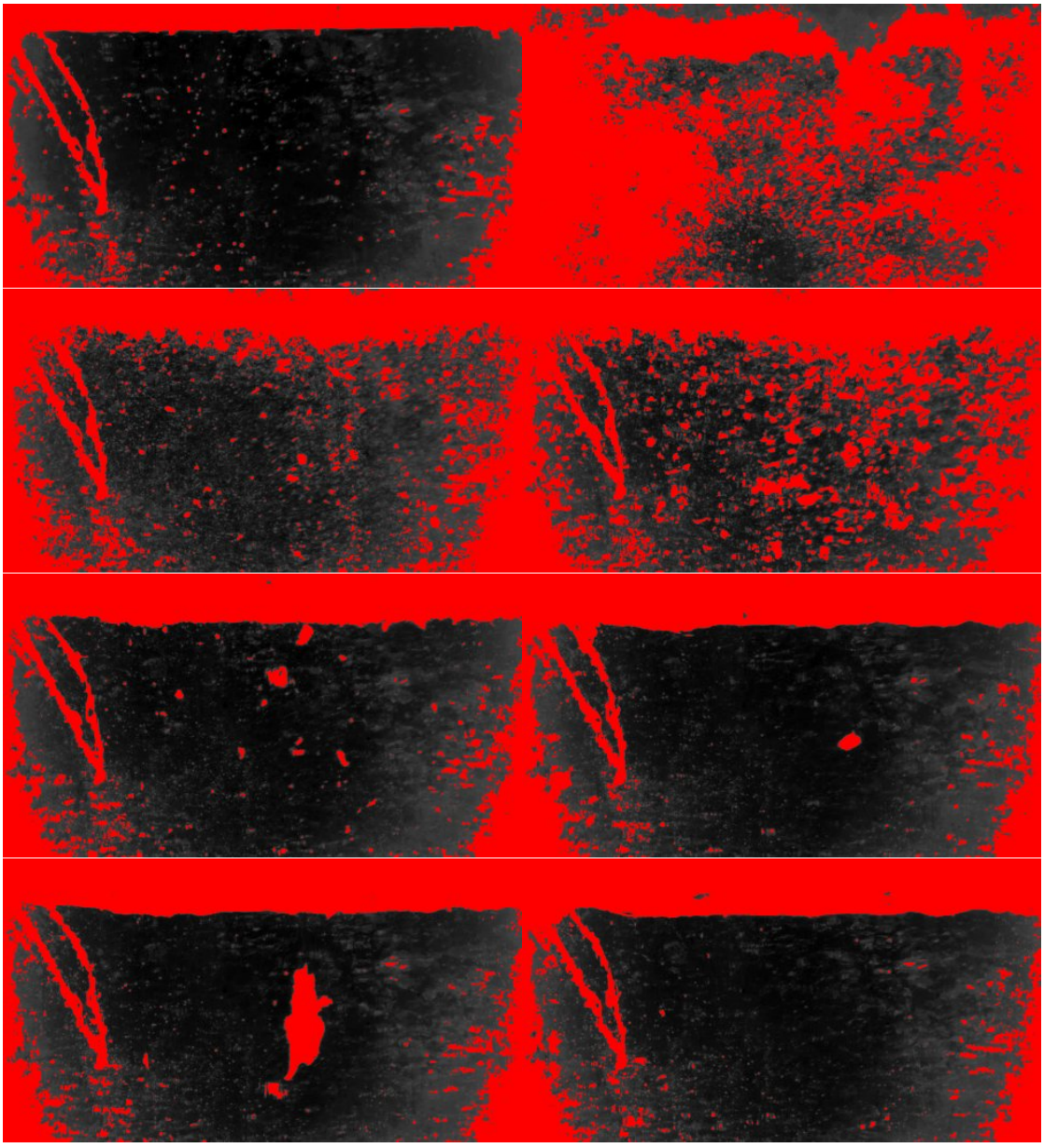

Figure 4.21: Figure 4.20 with applied Treshold on area marked in first picture

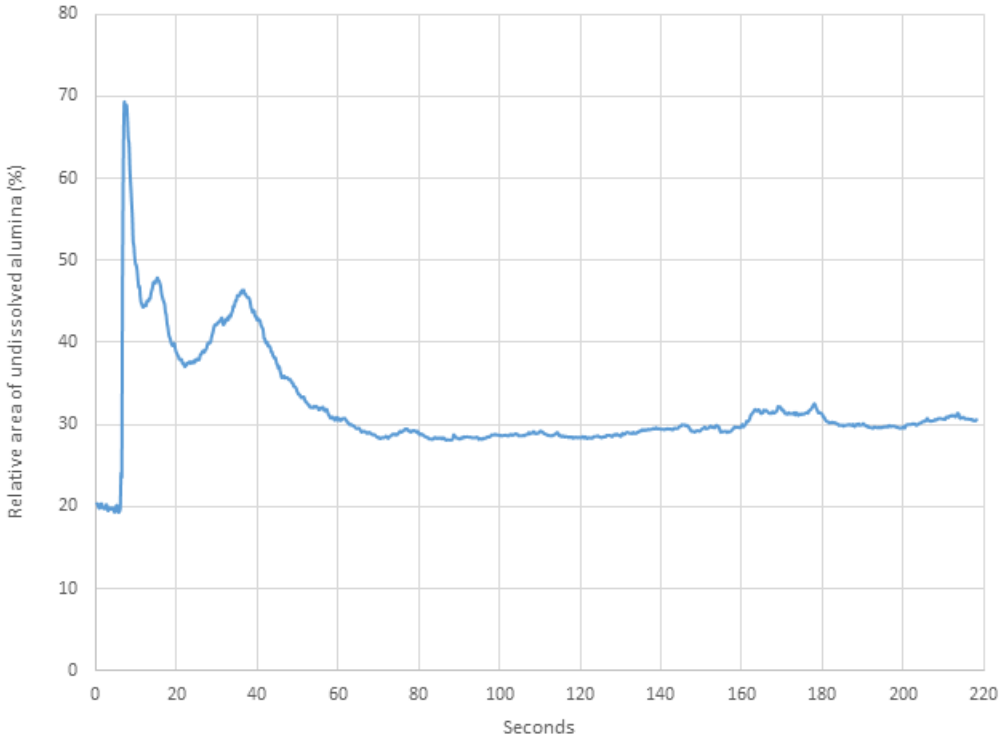

Figure 4.22: Graph showing the dissolution based on the treshold from figure 4.21

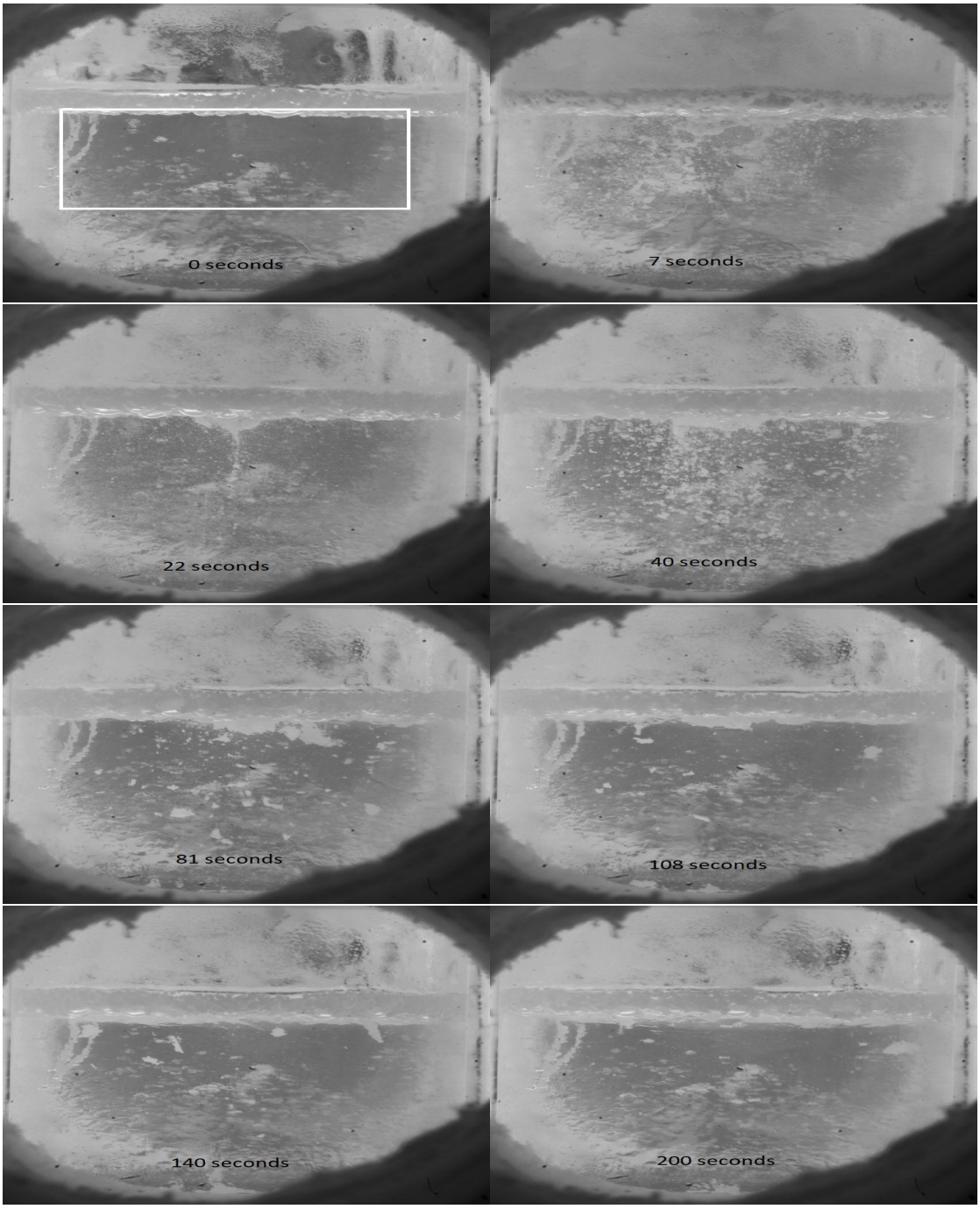

Figure 4.23: Pictures from third addition of secondary alumina with 0.5 wt% carbon in the bath done on 01.06.2021. Video available at `https://youtu.be/jx5gNMKlx0c`

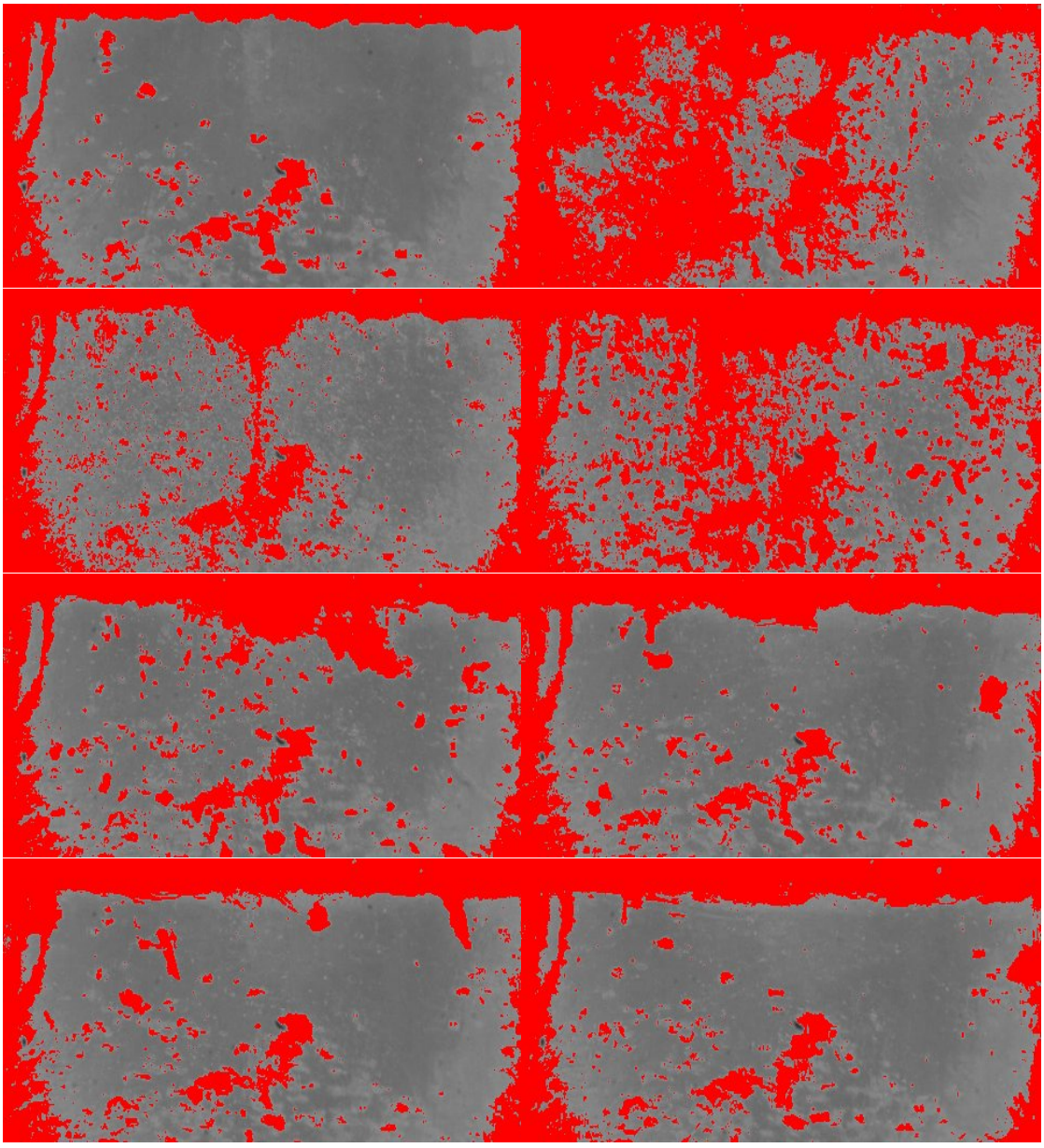

Figure 4.24: Figure 4.23 with applied Treshold on area marked in first picture

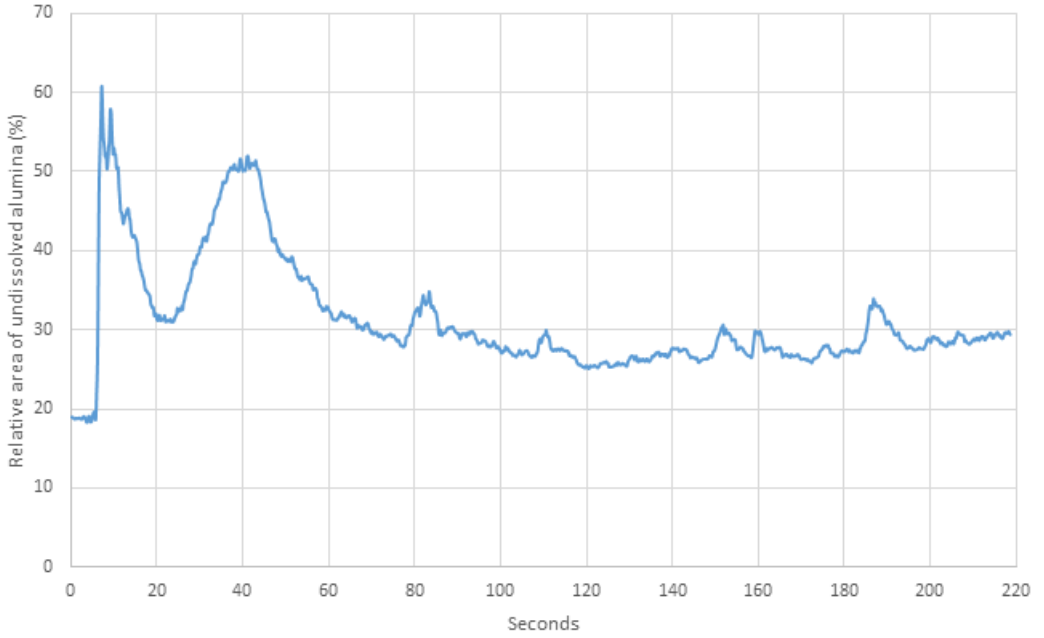

Figure 4.25: Graph showing the dissolution based on the treshold from figure 4.24

4.5 Dissolution times

The dissolution times for the different experiments were decided by looking at the videos taken by the Sony camera, which was able to film during the entire dissolution process. They are presented in the tables below.

Table 4.1: Dissolution times for standard experiments

Date	**Addition**	**Dissolution time**
14.04	1	18 minutes
14.04	2	¿13 minutes (video stops)
16.04	1	12 minutes
16.04	2	16 minutes (larger dose)
16.04	3	14 minutes and 30 seconds
16.04	4	15 minutes and 30 seconds
22.04	3	12 minutes and 10 seconds

Table 4.2: Dissolution times for sulfur experiments

Date	**Addition**	**Amount of Na_2SO_4**	**Dissolution time**
20.04	1	2 wt%	13 minutes
20.04	2	4 wt%	10 minutes and 20 seconds
20.04	3	2 wt%	8 minutes (uncertain)
20.04	4	4 wt%	11 minutes
22.04	1	5 wt%	4 minutes and 20 seconds
22.04	2	10 wt%	8 minutes and 10 seconds
22.04	4	5 wt%	8 minutes
03.06	1	20 wt%	3 minutes
03.06	2	4 wt%	3 minutes and 15 seconds
03.06	3	2 wt%	4 minutes
03.06	4	4 wt%	3 minutes

Table 4.3: Dissolution times for carbon experiments

Date	**Addition**	**Carbon in bath**	**Dissolution time**	**Temperature**
26.05	1	1 wt%	26 minutes	No measurement
26.05	2	1 wt%	22 minutes	960 °C
26.05	3	1 wt%	24 minutes	962 °C
26.05	4	1 wt%	20 minutes (uncertain)	961 °C
28.05	1	0.1 wt%	11 minutes	953 °C
28.05	2	0.1 wt%	5 minutes	956 °C
28.05	3	0.1 wt%	7 minutes	957 °C
28.05	4	0.1 wt%	7 minutes	958 °C
01.06	1	0.5 wt%	16 minutes	958 °C
01.06	2	0.5 wt%	11 minutes	961 °C
01.06	3	0.5 wt%	8 minutes	963 °C
01.06	4	0.5 wt%	9 minutes	962 °C

5 Discussion

5.1 Experimental setup

The experimental setup used for this Master's thesis was a big improvement compared to the project work. Experiments on the same see through cell during the project work was done with a window on only one of the openings of the furnace causing a big heat loss [18]. The change from a molten bath of pure synthetic cryolite to a bath based on an industrial bath also gave much better sight in the crucible.

Another change was to get fixed windows on the oven instead of removable shutters. In the project work and the initial experiments, the oven still had shutters that had to be replaced by windows during the experiment when addition of alumina occurred. This affected the heat balance for the cryolite several times during the experiments, which led to freezing of the bath.

5.2 Image processing

ImageJ worked well for the videos taken with the high-speed camera. The high speed camera had sharp images but could only film for 218 seconds, which was not long enough to see the full dissolution process for most of the experiments. For the faster dissolution experiments the treshold graphs gave a good indication of when the dissolution process would be finished. For the slower dissolution experiments the treshold graph can still be useful in showing the raft formation, as for the graph in figure 4.22. The percentage that the graph stabilizes on after the initial dissolution subtracted with the background noice which is shown in the graph where no addition has occurred yet will give an idea of how large the raft is.

Applying treshold on the videos taken by the Sony camera provided more difficulties. The image processing was largely influenced by lighting conditions leading to problems with reflections on the crucible. Fumes within the oven were more evident on the videos from the Sony camera.

The image processing method shows a lot of promise, especially for the faster dissolutions. Figures 4.16 to 4.18 shows the dissolution process for the fourth addition experiment at 03.06.21 where 4 wt% sulfur was mixed with alumina. As can be seen from the graph the the treshold figure the crucible surface is back at starting position after 3 minutes.

5.3 Initial experiments

The initial experiments was done with a cryolite mixture consisting of synthetic cryolite as base with additions like AlF_3 and CaF_2 to mimic the properties of industrial baths. These experiments was also used as a comparison for primary and secondary alumina dissolution as done by [23] and [24] earlier. The dissolution processes can be seen in figures 4.1, 4.2 and 4.3. The dissolution experiments gave clear pictures, but also had some issues.

A big problem with the initial experiments was that the cryolite melted really slowly and required a really high set temperature on the oven to be clear enough for visible dissolution experiments. A long melting time will have a severely negative impact on the experiment as the crucible has a limited 'survival time' at high temperatures with cryolite inside. This led to days where only two dissolution experiments was possible before the crucible had visible holes and further additions probably would lead to total destruction of the crucible as shown in figure 2.18 and possibly damages to the oven.

5.4 Establishing a standard

The standard experiments was meant to be a source for comparison for the other experiments. This was somewhat achieved, but the standard experiments also became trial experiments for the new industrial bath. The first standard experiment on 14.04 was done with 3 % excess LiF, which led to a long melting time for the bath similarly with the initial experiments. The second experiment on 16.04 was done with 4 % excess LiF, which improved the melting time but a further increase was decided leaving the two standard experiments as the only ones not done with 5 % excess LiF.

5.5 Sulfur

The experiments done with sodium sulfate mixed with the alumina had faster dissolution times than the standard experiments, as expected from the theory. Sodium sulfate is not stable as a powder at the high temperatures in the bath, leading to the destruction of the formed alumina rafts more quickly. As discussed in the literature study, the formation of the intermediate compound $Al_2(SO_4)_3$ described by equation 2.1 and further decomposing to Al_2O_3 and SO_2 [14], could be a reaction influencing the raft dissolution.

As described by Meirbekova et al. [16] the factors that had the biggest impact on removal of sodium sulfate were electrolysis, followed by the presence of carbon and aluminium in the cell. In the experiments done in this project none of this factors

were available, suggesting a rather slow depletion of sodium sulfate as described in figure 2.5. Doing CT analysis of rafts created in sulfur experiments as described by Gylver et al. [26] could give insight into the effect of gas evolution within the raft.

Despite the experiments showing a decreased dissolution time with added sodium sulfate to the alumina, more sulfur in the cells is negative for the current efficiency as reported by Pietrzyk et al. [6]. Additionally the environmental impact from increasing the amount of sulfur in the electrolysis cells could be a big drawback.

5.6 Carbon

Carbon has a lower density than the bath, and for the experiments with carbon mixed in the bath it was expected that most of the carbon would lay upon the surface. As described by Fossnæs et al. [19] some carbon particles were found throughout the bath, but most of the larger particles were found in the upper layer. The videos from the carbon experiments seemed to show particles laying on the surface, which is in agreement with the theory.

The dissolution times for experiments done with various amounts of carbon mixed in the bath showed mixed results. Some of the experiments done on 28.05 with 0.1 wt% carbon in the bath had really fast dissolution times, even faster than the standard experiments. On the other hand, experiments done on 26.05 with 1 wt% carbon in the bath had very slow dissolution times. Carbon dust on the surface will lead to a layer which somewhat delays the wetting of the added alumina, making a larger part of the added alumina freeze and form a raft.

Another problem with the carbon as a layer was that it made it more difficult to determine when the rafts were fully dissolved. There was always some carbon on the upper layer of the bath, and distinguishing between carbon and raft was not always easy. The carbon experiments were also the only experiment done with a thermocouple measuring the temperature in the surface area of the melt. The temperatures are given

5.7 Uncertainties

Due to the automatic processing method not working on the videos showing the whole dissolution process the dissolution times are less certain. When the dissolution times are a lot longer than the duration the high speed camera could film, the automatic processing method are of very little help. In those cases only visual observations from videos could be used to determine dissolution times.

As see through cells are somewhat open environments, operational conditions could vary a lot even if some parameters like bath composition are kept constant. One of this operational conditions was the temperature in the bath. Some experiments was performed with a thermocouple in the melt which gives us the temperature in the surface area of the bath. If the temperature of the melt is too low it could negatively impact the dissolution as less of the alumina dissolve immediately. As the dissolution times often fluctuated even within the same day temperature measurement could have given valuable information. A thermocouple was not available for the sulphur experiments and data from the thermocouple in the standard experiments could not be gathered.

6 Conclusion and Further work

30 experiments have been conducted in a see through furnace in order to assess the influence of sulfur in alumina and carbon dust in the bath on dissolution times. Most experiments with carbon dust indicate show longer dissolution times, most likely due to inadequate wetting conditions between bath and alumina on the bath surface where dust is accumulated. For sulfur, here added as sulphate, in the alumina, the dissolution process appears to be enhanced, most likely due to additional gas evolution within the raft, resulting in an earlier disintegration and thereby a more effective dispersion.

The additional gas evolution could be confirmed by CT analysis of collected rafts under similar conditions, as described by Gylver et al. [26] for standard conditions. Raft extraction could also be used to quantify the size of the carbon film suggested here.

The lighting conditions in the furnace did not allow for automated postprocessing, making it challenging to extract quantitative data for the dissolution process. Reflections and fumes were particularly challenging as well as high concentrations of dust.

Enclosing the furnace and camera with a light-tight box could improve the challenges relating to reflections, but fumes are most likely challenging to control.

Based on the semi-qualitative results found in the current work, it appears as though dust has a greater influence on the dissolution process than that of sulfur in the alumina, even at elevated concentrations. As such, the industry should aim to maintain good operational practices for their cells in order to dissolve alumina as intended.

Dissolution experiments in see-through cells with automatic image processing shows a lot of promise, and should be attempted for other dissolution factors of interest. Further investigation into carbon dust as a factor affecting dissolution times could improve operations.

7 References

[1] K. Grjotheim and H. Kvande. *Introduction to aluminium electrolysis.* Alu media GmbH, Düsseldorf, 2 edition, 1993.

[2] M. P. Taylor P. Lavoie and J. B. Metson. A review of alumina feeding and dissolution factors in aluminum reduction cells. In *Metallurgical and Materials Transactions B*, volume 47, no. 4, pages 2690–2696. The Minerals, Metals & Materials Society and ASM International 2016, 2016.

[3] E. Skybakmoen, A. Solheim, and Å. Sterten. Alumina solubility in molten salt systems of interest for aluminium electrolysis and related phase diagram data. In *Metallurgical and Materials Transactions B*, volume 28 B, pages 81–86. 1997.

[4] Åste Hegglid Follo. Alumina dissolution in hall-hêroult cells. Project work, NTNU, 12 2018.

[5] R. K. Jain, S. B. Tricklebank, B. J. Welch, and D. J. Williams. Interaction of aluminas with aluminium smelting electrolysis. In *Light Metals 1983*, pages 609–622. Hoboken, 1983.

[6] S. Pietrzyk and J. Thonstad. Influence of the sulphur content in the carbon anodes in aluminium electrolysis, a laboratory study. In Carlos E. Suarez, editor, *Light Metals 2012*, pages 597–601. TMS (The Minerals, Metals & Materials Society, 2012.

[7] P. Fellner, J. Jurisova, V. Khandl, A. Sykorova, and J. Thonstad. Adsorption of SO_2 on alumina. 2006.

[8] W. D. Lamb. SO_2 in aluminum reduction-cell dry scrubbing systems. In *JOM (The Journal of The Minerals, Metals & Materials Society (TMS))*, volume 31, pages 32–37. 1979.

[9] Jana Hajasova. *Electrochemical behaviour of Sulphur containing species in molten salts.* PhD thesis, NTNU, Trondheim, 10 2007.

[10] M. Ambrova, P. Fellner, J. Gabcova, , and A. Sykorova. Chemical reactions of sulphur species in cryolite-based melts. 2004.

[11] P. Fellner, M. Korenko, M. Ambrova, V. Danielik, and J. Thonstad. Reactions of sulphides in molten cryolite. 2003.

[12] M. Ambrova, P. Fellner, J. Jurisova, and J. Thonstad. Determination of sulphur species in solidified cryolite melts. 2012.

[13] R. Oedegard, S. Roenning, A. Sterten, and J. Thonstad. Sulphur containing

compounds in the anode gas from aluminium cells, a laboratory investigation. In *Light Metals 1985*, pages 898–902. Hoboken, 1983.

[14] R. Souza, R. Navarro, A. V. Grillo, and E. Brocchi. Potassium alum thermal decomposition study under non-reductive and reductive conditions. In *Journal of Materials Research and Technology*, volume 8, pages 745–751. 2019.

[15] R. Meirbekova, G. M. Haarberg, J. Thonstad, and G. Saevarsdottir. Influence of sulfur species on current efficiency in the aluminum smelting process. In *Metallurgical and Materials Transactions B*, volume 47B, pages 1309–1314. The Minerals, Metals & Materials Society and ASM International 2016, 2016.

[16] R. Meirbekova, G. M. Haarberg, T. A. Aarhaug, and G. Saevarsdottir. Investigation of sodium sulfate additions into cryolite-alumina melts. In Edward Williams, editor, *Light Metals 2016*, pages 365–370. TMS (The Minerals, Metals & Materials Society) 2016, 2016.

[17] S. Pietrzyk, J. Thonstad, and A. Solheim. The effect of high contents of carbon dust in the electrolyte in aluminium electrolysis.

[18] Vegard Aulie. Dispersion and dissolution of alumina in cryolite melts: dissolution behavior in see-through cell. Project work, NTNU, 1 2019.

[19] T. Foosnæs, T. Naterstad, M. Bruheim, and K. Grjotheim. Anode dusting in hall-heroult cells. In R. E. Miller, editor, *Light Metals 1986*, pages 633–642. TMS (The Minerals, Metals & Materials Society, 2012.

[20] Louis Bugnion and Jean-Claude Fischer. Effect of carbon dust on the electrical resistivity of cryolite bath. In Edward Williams, editor, *Light Metals 2016*, pages 587–591. TMS (The Minerals, Metals & Materials Society, 2016.

[21] M. Dechent, M. P. Taylor, L. Tiedemann R. Meier, M. Meier, and B. Friedrich. Carbon dust - its short-term influence on potroom operations during anode change. In L. Perrander, editor, *Light Metals 2021*, pages 384–392. TMS (The Minerals, Metals & Materials Society, 2021.

[22] W.E. Haupin and W.C. Mcgrew. See-through hall-heroult cell. In *Essential Readings in Light Metals*, volume 2, pages 234–239. John Wiley and Sons, 2013.

[23] Yang et al. Study on the dissolution of alumina in cryolite electrolyte using the see-through cell. In Margaret Hyland, editor, *Light Metals 2015*, pages 541–546. Hoboken, NJ, USA: John Wiley & Sons, Inc., 2015.

[24] Q. Feng B. Gao and Z. Wang. The alumina dissolution in industrial aluminum cells. In *Journal of Siberian Federal University. Engineering & Technologies*, volume 11, pages 376–386. 2018.

[25] L. Bracamonte, E. Sandnes, V. Aulie, C. Rosenkilde, and K. E. Einarsrud. Dissolution characteristics and concentration measurements of alumina in cryolite melts. In L. Perrander, editor, *Light Metals 2021*, pages 495–503. TMS (The Minerals, Metals & Materials Society, 2021.

[26] S. E. Gylver, A. Solheim, H. Gudbrandsen, Å. H. Follo, and K. E. Einarsrud. Lab scale experiments on alumina raft formation. In A. Tomsett, editor, *Light Metals 2020*, pages 659–663. TMS (The Minerals, Metals & Materials Society, 2020.

Appendix

Sodium sulphate reactions in Hall-Hêroult cells

Reactions with carbon:

$$3\,Na_2SO_4 + 12\,C \longrightarrow 3\,Na_2S + 12\,CO \tag{7.1}$$

$$3\,Na_2SO_4 + \ + 2\,Na_3AlF_6 + 3\,C \longrightarrow 12\,NaF + Al_2O_3 + 3\,SO_2 + 3\,CO \tag{7.2}$$

$$3\,Na_2SO_4 + 2\,Na_3AlF_6 + \frac{3}{2}\,C \longrightarrow 12\,NaF + Al_2O_3 + 3\,SO_2 + \frac{3}{2}\,CO_2 \tag{7.3}$$

$$3\,Na_2SO_4 + \frac{21}{2}\,C + 2\,AlF_3 \longrightarrow 6\,NaF + Al_2O_3 + \frac{3}{2}\,CS_2 + 9\,CO \tag{7.4}$$

$$3\,Na_2SO_4 + 7\,C \longrightarrow CS_2 + 2\,Na_2O + 6\,CO \tag{7.5}$$

$$CS_2 + CO_2 \longrightarrow 2\,COS \tag{7.6}$$

Reactions with aluminium:

$$3\,Na_2SO_4 + 8\,Al \longrightarrow 4\,Al_2O_3 + 3\,Na_2S \tag{7.7}$$

$$3\,Na_2SO_4 + 8\,Al \longrightarrow 3\,Na_2O + 3\,Al_2O_3 + Al_2S_3 \tag{7.8}$$

$$3\,Na_2SO_4 + 2\,AlF_3 + 8\,Al \longrightarrow 6\,NaF + 4\,Al_2O_3 + Al_2S_3 \tag{7.9}$$

$$3\,Na_2SO_4 + 2\,Na_3AlF_6 + 8\,Al \longrightarrow 12\,NaF + 4\,Al_2O_3 + Al_2S_3 \tag{7.10}$$

$$Na_2S + Al_2O_3 \longrightarrow 2\,Al + SO_2 + Na_2O \tag{7.11}$$

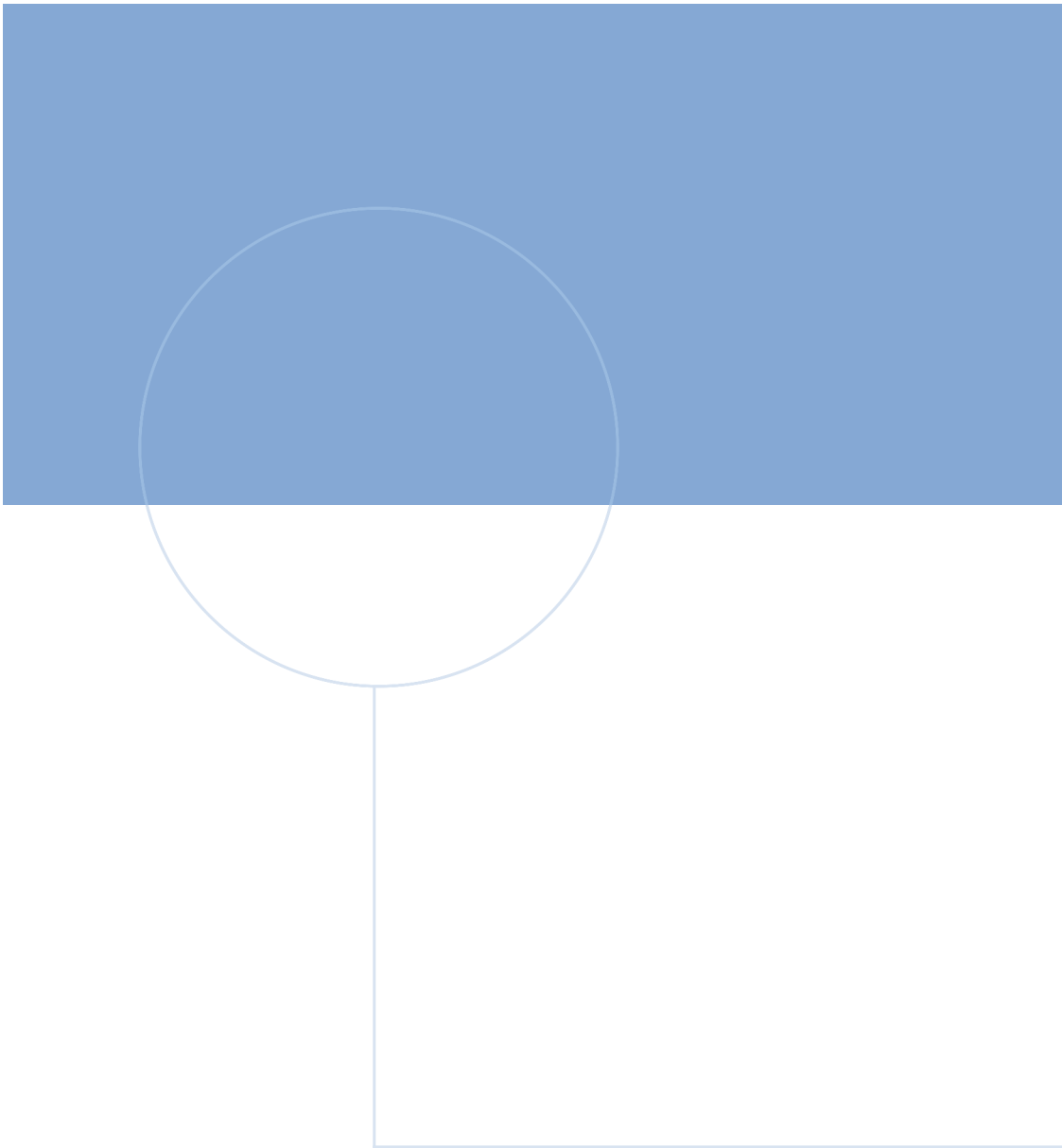

NTNU

Kunnskap for en bedre verden